

Electronic Supplementary Information

Luminescent 1D heterometallic (Ir,Cd) coordination polymers
based on *bis*-cyclometalated Ir(III) metallatectons and
trinuclear Cd(II) dianionic nodes

*Maxime Florent, Nathalie Kyritsakas, Jean-Marc Planeix, * Aurélie Guenet, * and Mir Wais
Hosseini**

Molecular Tectonics Laboratory, UMR UDS-CNRS 7140, icFRC, University of Strasbourg,
F-67000, Strasbourg, France

General.	S2
Synthesis	S4
NMR spectra of final complexes	S9
Crystallographic data	S14
References	S23

General.

NMR spectra were recorded on Bruker Avance AV300 (300 MHz for ^1H , 75 MHz for ^{13}C , 282 MHz for ^{19}F), Bruker Avance AV400 (400 MHz for ^1H , 100 MHz for ^{13}C) or Bruker Avance AV500 (500 MHz for ^1H , 125 MHz for ^{13}C , 470 MHz for ^{19}F) spectrometers at 20°C with complete proton decoupling for nucleus other than ^1H . Chemicals shifts (in ppm) were determined relative to residual undeuterated solvent as internal reference (CDCl_3 : 7.26 ppm for ^1H and 77.2 ppm for ^{13}C ; CD_3CN : 1.94 ppm for ^1H and 118.3 ppm and 1.3 ppm for ^{13}C). Spin multiplicities are given with the following abbreviations: s (singlet), br s (broad singlet), d (doublet), dd (doublet of doublet), t (triplet), q (quadruplet), m (multiplet) and coupling constants (J) quoted in Hz. ^1H NMR spectra were assigned by standard methods combined with COSY and NOESY/ROESY experiments. ^{13}C spectra were assigned by standard methods combined with DEPT, HMQC and HMBC experiments.

Mass spectrometry was performed at the “Service de spectrométrie de masse”, Université de Strasbourg. Low and high-resolution mass spectra (positive and negative mode ESI: Electro Spray Ionization) were recorded on Thermoquest AQA Navigator® with time of flight detector.

Elemental analyses were performed on a Thermo Scientific Flash 2000 by the “Service d’analyses, de mesures physiques et de spectroscopie optique”, Université de Strasbourg.

X-ray crystal structure data were collected on a Bruker SMART CCD diffractometer with Mo-K α radiation. The structures were solved and refined using the Bruker SHELXTL Software Package using SHELXS-97 (Sheldrick, 2008) and refined by full matrix least squares on F^2 using SHELXL-97 (Sheldrick, 2014) with anisotropic thermal parameters for all non-hydrogen atoms.^{1,2} The hydrogen atoms were introduced at calculated positions and not refined (riding model). CCDC 1980611-1980615 and 1980617-1980621 contains the supplementary crystallographic data for this paper. These data can be obtained free of charge from the Cambridge Crystallographic Data Centre via www.ccdc.cam.ac.uk/data_request/cif.

Powder X-ray diffraction (PXRD) patterns were recorded on a Bruker D8 AV diffractometer using Cu-K α radiation ($\lambda = 1.5406 \text{ \AA}$) operating at 40 kV and 40 mA with a scanning range between 3.8 and 50° by a scan step size of 2°/min. For comparison, simulated patterns were calculated using the Mercury software.

UV/vis spectra in solution and in the solid state were recorded on a PerkinElmer Lambda 650S spectrophotometer (spectra in the solid state recorded in the reflection mode, using a 150 mm integrating sphere and Spectralon© as light spectral reference for the reflection

corrections). Wavelengths are given in nm and molar absorption coefficients (ϵ) are given in $\text{L}\cdot\text{mol}^{-1}\cdot\text{cm}^{-1}$. Spectrophotometric grade solvents were used for measurements.

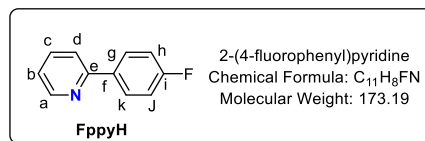
Steady state emission spectra of the discrete complexes were recorded in the solid state (powder samples) on a PicoQuant FluoTime 300 (PicoQuant GmbH, Germany) and corrected by standard correction curves. Time-resolved measurements were performed using either the time-correlated single-photon counting (TCSPC) electronics PicoHarp300 or the Multi-Channel Scaling (MCS) electronics NanoHarp 250 of the PicoQuant FluoTime 300 (PicoQuant GmbH, Germany), equipped with a PDL 820 laser pulse driver. A pulsed laser diode LDH-P-C-405 ($\lambda = 405$ nm, pulse FWHM <50 ps, repetition rate 200 kHz – 40 MHz) was used to excite the sample and mounted directly on the sample chamber at 90° . The photons were collected by a PMA-C-192 photomultiplier (PMT) single-photon-counting detector. The data were acquired by using the commercially available software EasyTau (PicoQuant GmbH, Germany), while data analysis was performed using the commercially available software FluoFit (PicoQuant GmbH, Germany). The absolute photoluminescence quantum yields (PLQY) of solids were measured on a Hamamatsu Quantaaurus-QY integrating sphere in air-equilibrated condition at room temperature using scan mode (300-400 nm, 10 nm step). Steady-state emission spectra of the coordination polymers were recorded in the solid state (powder samples) on a PerkinElmer LS55 spectrometer equipped with a Hamamatsu R928 photomultiplier tube. Emission and excitation spectra were corrected for source intensity (lamp and grating) and emission spectral response (detector and grating) by standard correction curves.

Synthesis. All air sensitive and anhydrous reactions were carried out under argon. Light sensitive reactions were protected from light by covering with aluminium foil. The glassware was oven dried at 100°C and cooled under argon flow. Commercially available chemicals were used without further purification. Anhydrous toluene, dichloromethane and CH_3CN were used as supplied by commercial sources without further purification.

Synthesis

FppyH

According to the procedure already reported,³ 2-bromopyridine (0.9 ml, 9.52 mmol, 1 eq), 4-fluorophenylboronic acid (2.00 g, 14.28 mmol, 1.5 eq), Pd(PPh₃)₄ (110 mg, 0.095 mmol, 0.01 eq) and K₂CO₃ (2.62 g, 18.0 mmol, 1.9 eq) were reacted together under argon in EtOH (40 mL). The work up procedure was slightly modified. The dark reaction mixture obtained after reaction was evaporated to dryness, dissolved in CH₂Cl₂ (100 ml) and washed with water (2 x 50 ml). The crude product was purified by Kugelrohr distillation (125 °C, 0.56 mbar). A colorless solid was obtained (1.60 g, 97 %).



¹H NMR (CDCl₃, 500 MHz, CDCl₃) δ (ppm): 8.67 (dt, J = 4.8, 1.4 Hz, 1H), 8.01 - 7.94 (m, 2H), 7.75 (td, J = 7.7, 1.8 Hz, 1H), 7.68 (dt, J = 8.1, 1.2 Hz, 1H), 7.23 (ddd, J = 7.4, 4.9, 1.2 Hz, 1H), 7.15 (m, 2H).

¹⁹F NMR (470 MHz, CDCl₃) δ (ppm): -113.2 (s).

¹³C NMR (125 MHz, CDCl₃) δ (ppm): 163.6 (d, ¹J_{C-F} = 248.4 Hz, C_{quat}), 156.6 (C_{quat}), 149.8 (CH), 137.0 (CH), 135.5 (d, ⁴J_{C-F} = 3.1 Hz, C_{quat}), 128.7 (d, ³J_{C-F} = 8.4 Hz, CH), 122.2 (CH), 120.4 (CH), 115.6 (d, ²J_{C-F} = 21.6 Hz, CH).

MS (ESI⁺): calcd for [M+H]⁺ (C₁₁H₉FN) 174.0714, found 174.0718

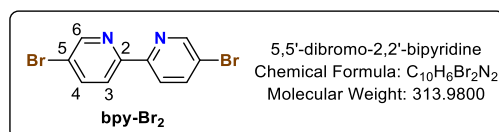
L2 was synthesized as previously described in 69 % yield.⁴

¹H NMR (CDCl₃, 500 MHz) δ (ppm): 8.70 (d, 2H, ⁴J = 2.4 Hz, H₆), 8.29 (d, 2H, ³J = 8.6 Hz, H₃), 7.93 (dd, 2H, ³J = 8.6 Hz, ⁴J = 2.4 Hz, H₄).

¹³C NMR (CDCl₃, 125 MHz) δ (ppm): 153.8 (C_{quat}), 150.4 (CH), 139.7 (CH), 122.3 (CH), 121.5 (C_{quat})

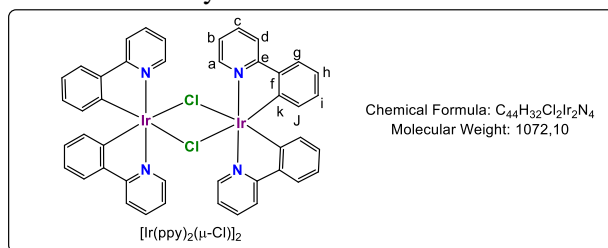
IR: ν cm⁻¹ 1544, 1455 (C=N), 1357, 1261, 1233, 1124, 1087, 1007, 827, 801, 726, 702, 638 (C-Br).

Elem. Anal. Calcd for C₁₀H₆Br₂N₂: C, 38.25, H, 1.93, N, 8.92. Found: C, 38.16, H, 2.12, N, 8.57.



[Ir(ppy)₂(μ-Cl)]₂ was synthesized as previously described in 76 % yield.⁵

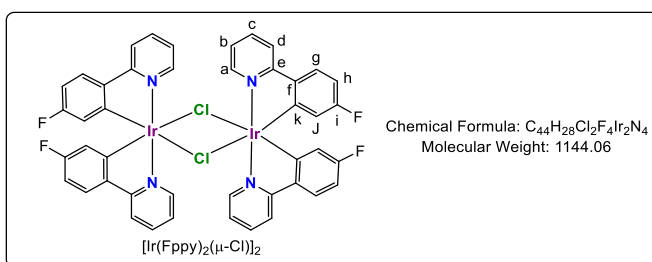
¹H NMR (CDCl₃, 300 MHz) δ (ppm): 9.24 (dd, 4H, ³J = 5.7 Hz, ⁴J = 1.0 Hz), 7.86 (d, 4H, ³J = 7.8 Hz), 7.73 (td, 4H, ³J = 7.5 Hz, ⁴J = 1.5 Hz), 7.48 (dd, 4H, ³J = 7.8 Hz, ⁴J = 1.2 Hz), 6.73-6.78 (m, 8H), 6.56 (ddd, 4H, ³J = 8.0 Hz, ³J = 8.0 Hz, ⁴J = 1.4 Hz), 5.93 (dd, 4H, ³J = 7.7 Hz, ⁴J = 1.0 Hz).



¹³C NMR (CDCl₃, 75 MHz) δ (ppm): 168.6 (C_{quat}), 151.7 (CH), 145.4 (C_{quat}), 143.7 (C_{quat}), 136.1 (CH), 130.6 (CH), 124.1 (CH), 123.7 (CH), 122.1 (CH), 121.3 (CH) 118.3 (CH).

[Ir(Fppy)₂(μ-Cl)]₂:

The reaction was performed under argon. The solvents were degassed by bubbling argon prior to reaction. IrCl₃·xH₂O (518 mg, 1.47 mmol, trihydrate basis, MW = 352.6) and FppyH (560 mg, 3.23 mmol, 2.2 eq) were dissolved into a 2-EtOEtOH/H₂O mixture (21 mL/7 mL) and the resulting



solution was heated at 120 °C overnight. After cooling, the yellow precipitate was filtered and washed successively with EtOH (10 mL), H₂O (10 mL), EtOH (10 mL), Et₂O (10 mL). The fine yellow powder was dried and used without further purification (612 mg, 73 %).

¹H NMR (CDCl₃, 300 MHz) δ (ppm): 9.13 (ddd, 4H, ³J = 5.8 Hz, ⁴J = 1.5 Hz, ⁵J = 0.9 Hz, H_a), 7.88-7.69 (m, 8H, H_c and H_d), 7.50 (dd, 4H, ³J = 8.6 Hz, ⁴J_{H-F} = 5.7 Hz, H_e), 6.80 (ddd, 4H, ³J = 7.2 Hz, ³J = 5.8 Hz, ⁴J = 1.5 Hz, H_b), 6.56 (td, 4H, ³J = 8.7 Hz, ³J_{H-F} = 8.7 Hz, ⁴J = 2.5 Hz, H_h), 5.53 (dd, 4H, ³J_{H-F} = 10.0 Hz, ⁴J = 2.5 Hz, H_j).

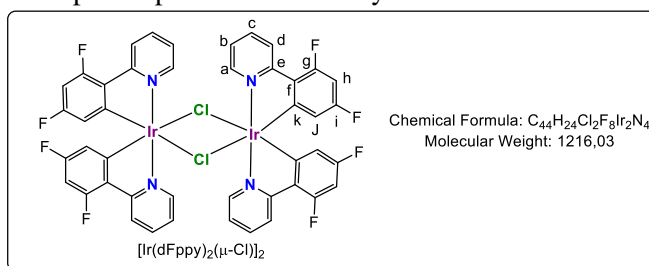
¹⁹F NMR (CDCl₃, 282 MHz) δ (ppm) -110.4 (s).

¹³C NMR (CDCl₃, 75 MHz) δ (ppm): 167.4 (C_{quat}), 162.8 (d, ¹J_{C-F} = 243.5 Hz, C_{quat}), 151.32 (CH), 147.3 (C_{quat}), 139.9 (d, J_{C-F} = 1.9 Hz, C_{quat}), 136.7 (CH), 125.4 (d, J_{C-F} = 9.7 Hz, CH), 122.2 (CH), 118.6 (CH) 116.6 (d, J_{C-F} = 18.4 Hz, CH), 108.9 (d, J_{C-F} = 23.2 Hz, CH).

MS (ESI⁺): calcd for [M]⁺ (C₄₄H₂₈Cl₂F₄Ir₂N₄) 1144.09, found 1144.08.

[Ir(dFppy)₂(μ-Cl)]₂ was synthesized following the reported procedure in 71% yield.⁶

¹H NMR (CDCl₃, 300 MHz) δ (ppm): 9.12 (dd, 4H, J = 5.7 Hz, J = 1.0 Hz), 8.31 (d, 4H, J = 8.3 Hz), 7.83 (td, 4H, J = 7.8 Hz, J = 1.3 Hz), 6.83 (ddd, 4H, ³J_{H-H} = 7.2 Hz, ³J_{H-H} = 7.2 Hz, ⁴J_{H-H} = 1.2 Hz), 6.33 (ddd, 4H, ³J_{H-F} = 12.6 Hz, ³J_{H-F} = 9.2 Hz, ⁴J_{H-H} = 2.4 Hz), 5.28 (dd, 4H, ³J_{H-F} = 9.3 Hz, ⁴J_{H-H} = 2.4 Hz).



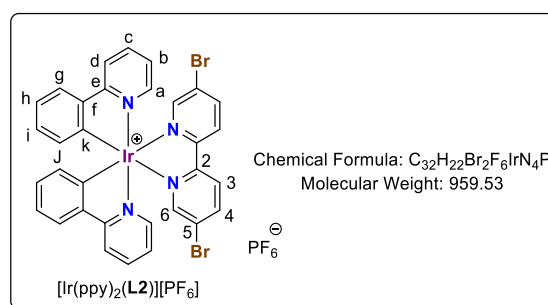
¹⁹F NMR (CDCl₃, 282 MHz) δ (ppm): -107.72 (d, 4F, ⁴J_{F-F} = 10.2 Hz), -110.32 (d, 4F, ⁴J_{F-F} = 10.2 Hz).

¹³C NMR (CDCl₃, 125 MHz) δ (ppm): 165.3 (d, ²J_{C-F} = 6.7 Hz, C_{quat}), 162.4 (dd, ¹J_{C-F} = 253.5 Hz, ³J_{C-F} = 12.9 Hz, C_{quat}), 160.4 (dd, ¹J_{C-F} = 253.5 Hz, ³J_{C-F} = 12.9 Hz, C_{quat}), 151.3 (CH), 147.6 (d, ³J_{C-F} = 7.1 Hz, C_{quat}), 137.6 (CH), 127.8 (C_{quat}), 122.7 (d, ⁴J_{C-F} = 19.9 Hz, CH), 122.6 (CH), 112.7 (d, ²J_{C-F} = 18.2 Hz, CH), 98.2 (t, ²J_{C-F} = 26.5 Hz, CH).

Elem. Anal: calcd for C₄₄H₃₂Cl₂Ir₂N₄·H₂O: C, 42.83, H, 2.12, N, 4.54. Found: C, 42.65, H, 2.20, N, 4.23.

[Ir(ppy)₂(L2)][PF₆] was synthesised adapting the procedure described for similar compounds.⁷

To a solution of [Ir(ppy)₂(μ-Cl)]₂ (50 mg, 0.047 mmol, 1 eq) in a 1/1 MeOH/DCM mixture (3 mL/3 mL) was added L2 (34 mg, 0.108 mmol, 2.3 eq). The yellow solution was heated at 60 °C overnight. Water (50 mL) was then added and the resulting solution was washed with diethyl ether (2x30 mL). The aqueous layer was heated to 70 °C and a solution of KPF₆ (100 mg in 5 mL water) was added. A yellow precipitate formed immediately. The aqueous solution was cooled using an ice bath for 2 hours, then filtered and washed with water (5 mL) and Et₂O (5 mL). The product was obtained as an orange powder (75 mg, 83%) by recrystallization from acetonitrile (2 mL) and diethyl ether (20 mL).



¹H NMR (CD₃CN, 300 MHz) δ (ppm): 8.40 (d, 2H, ³J = 8.7 Hz, H₃), 8.29 (dd, 2H, ³J = 8.8 Hz, ⁴J = 2.2 Hz, H₄), 8.07 (d, ³J = 8.1 Hz, H_d), 7.91 (d, 2H, ⁴J = 1.9 Hz, H₆), 7.87 (m, 2H, H_c), 7.82 (dd, 2H, ³J = 7.8 Hz, ⁴J = 0.9 Hz, H_g), 7.65 (m, 2H, H_a), 7.09-7.04 (m, 4H, H_b, H_h), 6.94 (td, 2H, ⁴J = 7.4 Hz, ³J = 1.3 Hz, H_i), 6.25 (dd, 2H, ³J = 7.6 Hz, ⁴J = 1.3 Hz, H_j).

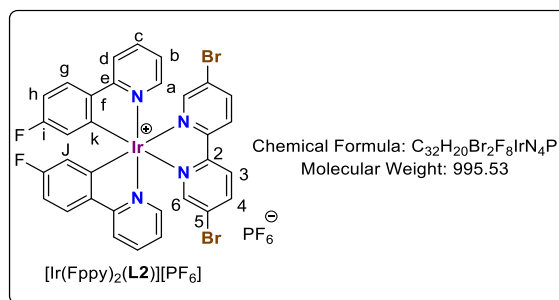
¹³C NMR (CD₃CN, 125 MHz) δ (ppm): 167.9 (C_{quat}), 154.9 (C_{quat}), 152.5 (CH), 150.6 (CH), 149.7 (C_{quat}), 145.0 (C_{quat}), 142.9 (CH), 139.7 (CH), 132.4 (CH), 131.4 (CH), 126.9 (CH), 125.9 (CH), 125.7 (C_{quat}), 124.6 (CH), 123.9 (CH), 121.0 (CH).

MS (ESI⁺): calcd for [M-PF₆]⁺ (C₃₂H₂₂Br₂Ir₁N₄) 812.98, found 812.98

UV-Visible (CH₂Cl₂) λ (nm), ε (10³ L.mol⁻¹.cm⁻¹): 268 (48.4), 288 (38.9), 331 (24.0), 380 (7.0), 401 (5.8).

[Ir(Fppy)₂(L2)][PF₆]:

To a solution of [Ir(Fppy)₂(μ-Cl)]₂ (500 mg, 0.45 mmol, 1 eq) in a mixture of MeOH/CH₂Cl₂ (20 mL/20 mL) was added L2 (295 mg, 0.94 mmol, 2.1 eq). The yellow solution was heated at 60 °C overnight. After evaporation to dryness, the mixture was dissolved in MeOH (50 mL) and heated at 70 °C. An aqueous KPF₆ solution (sat) (10 mL) was added. A yellow precipitate formed immediately. The suspension was placed in an ice bath for 2 hours before it was filtered, washed with H₂O (10 mL) and Et₂O (10 mL). The desired compound was obtained as a yellow powder (815 mg, 91 %).



¹H NMR (CD₃CN, 300 MHz) δ (ppm): 8.40 (d, 2H, ³J_{H-H} = 8.6 Hz, H₃), 8.31 (dd, 4H ³J = 8.8 Hz, ⁴J_{H-H} = 2.2 Hz, H₄), 8.05 (d, 2H, ³J_{H-H} = 8.2 Hz, H_a) 7.86-7.93 (m, 6H, H₆, H_b, H_g), 7.62 (d, 2H, ³J_{H-H} = 5.7 Hz, H_d), 7.07 (ddd, 2H, ³J_{H-H} = 7.4 Hz, ³J = 5.9 Hz, ⁴J_{H-H} = 1.5 Hz, H_c), 6.85 (td, 2H, ³J_{H-F} = 8.9 Hz, ⁴J_{H-H} = 2.6 Hz, H_h), 5.85 (dd, 2H, ³J_{H-F} = 9.5 Hz, ⁴J_{H-H} = 2.6 Hz, H_j).

¹⁹F NMR (CD₃CN, 282 MHz) δ (ppm): -73.9 (d, 6F, ¹J_{P-F} = 707 Hz, PF₆), -111.6 (s, 2F).

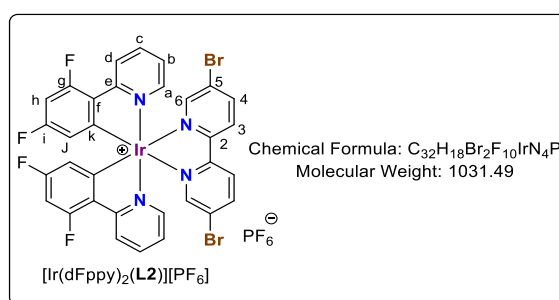
¹³C NMR (CD₃CN, 125 MHz) δ (ppm): 166.8 (C_{quat}), 164.4 (d, ¹J_{C-F} = 252.8 Hz, C_{quat}) 154.7 (C_{quat}), 152.6 (CH), 152.5 (d, J_{C-F} = 5.9 Hz, C_{quat}), 150.7 (CH), 143.2 (CH), 141.4 (d, J_{C-F} = 2.0 Hz, C_{quat}), 140.0 (CH), 128.2 (d, J_{C-F} = 9.5 Hz, CH), 126.9 (CH), 125.8 (C_{quat}), 124.5 (CH), 121.2 (CH), 117.9 (d, J_{C-F} = 18.2 Hz, CH), 110.9 (d, J_{C-F} = 23.3 Hz, CH).

HRMS (ESI⁺): calcd for [M-PF₆]⁺ C₃₂H₂₀Br₂F₂Ir₁N₄ 850.96, found 850.96.

UV-Visible (THF): λ (nm), ε (10³ L.mol⁻¹.cm⁻¹) 269 (43.4), 317 (24.4), 328 (22.5, s), 365 (6.9) (s).

[Ir(dFppy)₂(L2)][PF₆] was synthesized as previously reported.⁸

To a solution of [Ir(dFppy)₂(μ-Cl)]₂ (0.22 g, 0.18 mmol, 1 eq) in a mixture of MeOH/CH₂Cl₂ (5 mL/5 mL), L2 (0.12 g, 0.37 mmol, 2.05 eq) was added. The yellow solution was heated at 60 °C overnight. After cooling, water (30 mL) was added and the aqueous layer was washed with Et₂O (2x30 mL). After heating the aqueous layer at 70 °C, an aqueous KPF₆ solution (100 mg in 5 mL H₂O) was added. A yellow precipitate formed immediately, and the suspension was placed in an ice bath for 2 hours. The suspension was filtered, washed with H₂O (5 mL) and ether (5 mL). The desired compound was obtained as a yellow powder (0.23 g, 60 %) after recrystallization from acetonitrile (2 mL) and diethylether (20 mL).



¹H NMR (CD₃CN, 300 MHz) δ (ppm): 8.43 (d, 2H, ³J = 8.6 Hz, H₃), 8.34-8.31 (m, 4H, H₄, H_{a/d}), 7.96-7.91 (m, 4H, H₆ and H_{b/c}), 7.67 (d, 2H, ³J = 5.7 Hz, H_{a/d}), 7.11 (ddd, 2H, ³J = 7.5 Hz, ³J = 5.8 Hz, ⁴J = 1.3 Hz, H_{b/c}), 6.71 (ddd, 2H, ³J_{H-F} = 12.4 Hz, ³J_{H-F} = 9.0 Hz, ⁴J = 2.5 Hz, H_h), 5.68 (dd, 2H, ³J_{H-F} = 8.8 Hz, ⁴J = 2.3 Hz, H_j).

¹⁹F NMR (CD₃CN, 282 MHz) δ (ppm): -73.9 (d, 6F, ¹J_{P-F} = 706 Hz, PF₆), -108.8 (d, 2F, ⁴J_{F-F} = 10.7 Hz), -110.7 (d, 2F, ⁴J_{F-F} = 10.7 Hz).

¹³C NMR (CD₃CN, 125 MHz) δ (ppm): 164.3 (dd, ¹J_{C-F} = 253 Hz, ²J_{C-F} = 13.3 Hz, C_{g/i}), 164.3 (d, J_{C-F}

= 7.0 Hz, $C_{e/f}$), 162.1 (dd, $^1J_{C-F} = 260$ Hz, $^2J_{C-F} = 12.7$ Hz, $C_{g/i}$), 154.6 (C_5), 153.4 (d, $J_{C-F} = 6.7$ Hz, $C_{e/f}$), 152.7 (C_6), 151.0 ($C_{a/d}$), 143.6 (C_4), 140.6 ($C_{b/c}$), 129.0 (C_k), 127.0 (C_3), 126.0 (C_2), 124.9 ($C_{a/b/c/d}$), 124.8 ($C_{a/b/c/d}$), 114.8 (dd, $^3J_{C-F} = 18.1$ Hz, $^4J_{C-F} = 2.3$ Hz, C_j), 100.1 (t, $^3J_{C-F} = 26.8$ Hz, C_h).

HRMS (ESI⁺): calcd for $[M-PF_6]^+ C_{32}H_{18}Br_2F_4Ir_1N_4$ 884.9419, found 884.9308.

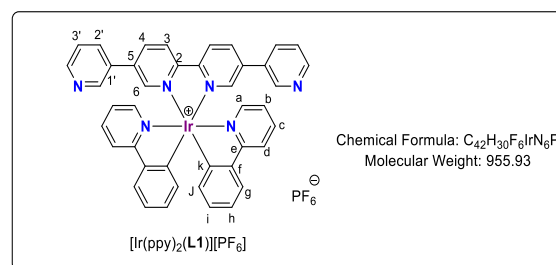
UV-Visible (THF): λ (nm), ϵ (10^3 L.mol⁻¹.cm⁻¹) 271 (63.1), 308 (s, 36.1), 330 (s, 23.8), 363 (s, 7.7).

General procedure for the Suzuki-coupled pyridyl derivatives:

To a solution of $[Ir(Xppy)_2(L_2)][PF_6]$ ($Xppy = ppy, Fppy$ or $dFppy$) (1eq) in a mixture of toluene/EtOH/H₂O/CH₃CN (1/1/1/1) was added 3-pyridinylboronic acid (2.2 eq). After degassing the resulting yellow solution with argon, Pd(PPh₃)₄ (0.22 eq) and K₂CO₃ (5.22 eq) were added and the solution was heated at 100 °C overnight. After filtration, CH₂Cl₂ (20 to 40 mL) was added and the organic layer was washed with water (2x 10 to 20 mL) and evaporated to dryness. Recrystallization by vapor diffusion of Et₂O into a CH₃CN or CHCl₃ solution containing the desired product afforded the different complexes as red to yellow solids.

$[Ir(ppy)_2(L_1)][PF_6]$:

$[Ir(ppy)_2(L_2)][PF_6]$ (200 mg, 0.210 mmol), 3-pyridinylboronic acid (56 mg, 0.456 mmol), Pd(PPh₃)₄ (50 mg, 0.44 mmol) and K₂CO₃ (140 mg, 1.01 mmol) were reacted together in a mixture of toluene/EtOH/H₂O/CH₃CN (40 mL) according to the general procedure described above. Recrystallization by slow diffusion of Et₂O (40 mL) into a CH₃CN solution (5 mL) afforded $[Ir(ppy)_2(L_1)][PF_6]$ as a red solid (177 mg, 88 %). Single crystals suitable for X-Ray diffraction were obtained by vapour diffusion of Et₂O (20 mL) into an acetonitrile solution containing the Ir complex (20 mg in 2 mL).



¹H NMR (CD₃CN, 400 MHz) δ (ppm): 8.67 (d, 2H, $^3J = 8.6$ Hz), 8.63 (dd, 2H, $^3J = 4.8$ Hz, $^4J = 1.6$ Hz), 8.57 (dd, 2H, $^4J = 2.4$ Hz, $^4J = 0.9$ Hz), 8.43 (dd, 2H, $^3J = 8.5$ Hz, $^4J = 2.2$ Hz), 8.19 (dd, 2H, $^4J = 2.1$ Hz, $^4J = 0.7$ Hz), 8.09 (dt, 2H, $^3J = 8.2$ Hz, $^4J = 1.2$ Hz), 7.87 (m, 4H), 7.79 (m, 4H), 7.45 (ddd, 2H, $^3J = 8.0$ Hz, $J = 4.9$ Hz, $^4J = 0.9$ Hz), 7.08 (m, 4H), 6.98 (td, 2H, $^3J = 7.4$ Hz, $^4J = 1.3$ Hz), 6.40 (dd, 2H, $^3J = 7.6$ Hz, $^4J = 1.1$ Hz).

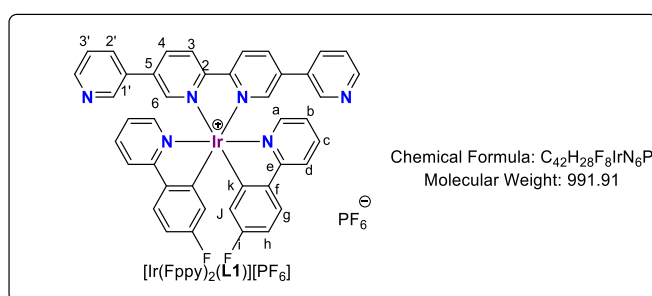
¹³C NMR (CD₃CN, 100 MHz) δ (ppm): 168.2 (C_{quat}), 155.6 (C_{quat}), 151.4 (CH), 150.9 (C_{quat}), 150.5 (CH), 149.5 (CH), 148.6 (CH), 145.2 (C_{quat}), 139.5 (CH), 138.7 (C_{quat}), 138.1 (CH), 135.3 (CH), 132.6 (CH), 131.8 (C_{quat}), 131.3 (CH), 125.9 (CH), 125.0 (CH), 124.6 (CH), 124.5 (CH), 123.6 (CH), 120.9 (CH).

MS (ESI⁺): calcd for $[M-PF_6]^+ C_{42}H_{30}Ir_1N_6$ 811.23, found 811.22.

UV-Visible (THF): λ (nm), ϵ (10^3 L.mol⁻¹.cm⁻¹) 256 (47.5), 266 (46.9), 296 (43.3), 338 (40.0), 405 (5.4).

$[Ir(Fppy)_2(L_1)][PF_6]$:

$[Ir(Fppy)_2(L_2)][PF_6]$ (200 mg, 0.210 mmol), 3-pyridinylboronic acid (54 mg, 0.44 mmol), Pd(PPh₃)₄ (51 mg, 0.44 mmol) and K₂CO₃ (140 mg, 1.05 mmol) were reacted together in a mixture of toluene/EtOH/H₂O/CH₃CN (40 mL) according to the general procedure described above. Recrystallization by diffusion of Et₂O (40 mL) into a CH₃CN solution (5 mL) afforded $[Ir(Fppy)_2(L_1)][PF_6]$ as an orange solid (159 mg, 82 %). Single crystals suitable for X-Ray diffraction were obtained by vapour diffusion



of Et₂O (20 mL) into an acetonitrile solution containing the Ir complex (20 mg in 3 mL).

¹H NMR (CD₃CN, 400 MHz) δ (ppm): 8.68 (d, 2H, ³J = 8.6 Hz), 8.64 (m, 4H), 8.45 (dd, 2H, ³J = 8.5 Hz, ⁴J = 2.2 Hz), 8.17 (d, 2H, ⁴J = 2.2 Hz), 8.04 (dt, 2H, ³J = 8.2 Hz, ⁴J = 1.1 Hz), 7.88 (m, 6H), 7.74 (m, 2H), 7.52 (ddd, 2H, ³J = 8.0 Hz, J = 4.9 Hz, ⁴J = 0.8 Hz), 7.07 (ddd, 2H, ³J = 7.4 Hz, ⁴J = 5.8 Hz, ⁴J = 1.4 Hz), 6.85 (td, 2H, ³J = 8.9 Hz, ⁴J = 2.6 Hz), 5.96 (dd, 2H, ³J = 9.5 Hz, ⁴J = 2.6 Hz).

¹⁹F NMR (CD₃CN, 282 MHz) δ (ppm): -73.9 (d, 6F, ¹J_{P-F} = 707 Hz, PF₆), -111.7 (s, 2F).

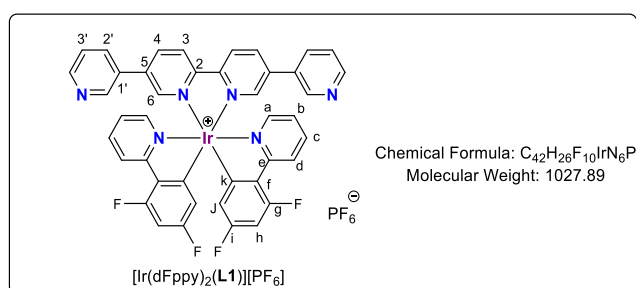
¹³C NMR (CD₃CN, 100 MHz) δ (ppm): 166.2 (C_{quat}), 163.7 (d, ¹J_{C-F} = 253 Hz, C_{quat}), 154.7 (C_{quat}), 152.7 (d, J_{C-F} = 5.8 Hz, C_{quat}), 149.7 (CH), 149.3 (CH), 148.8 (CH), 146.8 (CH), 140.7 (C_{quat}), 138.9 (CH), 137.7 (CH), 137.6 (C_{quat}), 135.9 (CH), 131.4 (C_{quat}), 127.2 (d, J_{C-F} = 9.3 Hz, CH), 125.2 (CH), 124.6 (CH), 123.6 (CH), 120.3 (CH), 117.6 (d, ¹J_{C-F} = 18.1 Hz, CH), 109.9 (d, J_{C-F} = 23.2 Hz, CH).

MS (ESI⁺): calcd for [M-PF₆]⁺ C₄₂H₂₈F₂Ir₁N₆ 847.20, found 847.19.

UV-Visible (THF): λ (nm), ε (10³ L.mol⁻¹.cm⁻¹) 253 (45.4), 268 (44.7), 293 (39.8), 340 (36.6), 396 (5.1) (s).

[Ir(dFppy)₂(L1)][PF₆]:

[Ir(dFppy)₂(L2)][PF₆] (200 mg, 0.19 mmol), 3-pyridinylboronic acid (52 mg, 0.42 mmol), Pd(PPh₃)₄ (51 mg, 0.044 mmol) and K₂CO₃ (140 mg, 1.05 mmol) were reacted together in a mixture of toluene/EtOH/H₂O/CH₃CN (40 mL) according to the general procedure described above. Recrystallization by diffusion



of Et₂O (50 mL) into a CHCl₃ solution (5 mL) afforded [Ir(dFppy)₂(L1)][PF₆] as an orange solid (150 mg, 77 %). Single crystals suitable for X-Ray diffraction were obtained by vapour diffusion of Et₂O (30 mL) into an acetonitrile solution containing the Ir complex (20 mg in 2 mL).

¹H NMR (CD₃CN, 400 MHz) δ (ppm): 8.70 (d, 2H, ³J = 8.5 Hz), 8.64 (m, 4H), 8.47 (dd, 2H, ³J = 8.5 Hz, ⁴J = 2.2 Hz), 8.31 (m, 2H), 8.18 (d, 2H, ⁴J = 2.1 Hz), 7.90 (td, 2H, ³J = 7.9 Hz, ⁴J = 0.9 Hz), 7.83 (dd, 2H, ³J = 8.5 Hz, ⁴J = 2.2 Hz), 7.80 (m, 2H), 7.45 (dd, 2H, ³J = 8.0 Hz, ⁴J = 4.8 Hz), 7.11 (ddd, 2H, ³J = 7.4 Hz, ⁴J = 5.8 Hz, ⁴J = 1.4 Hz), 6.71 (ddd, 2H, ³J_{H-F} = 12.3 Hz, ⁵J_{H-F} = 9.4 Hz, ⁴J = 2.4 Hz), 5.79 (dd, 2H, ²J_{H-F} = 8.6 Hz, ⁴J = 2.4 Hz).

¹⁹F NMR (CD₃CN, 282 MHz) δ (ppm): -73.9 (d, 6F, ¹J_{P-F} = 707 Hz, PF₆), -108.8 (d, 2F, ⁴J_{F-F} = 10.8 Hz), -110.8 (d, 2F, ⁴J_{F-F} = 10.8 Hz).

¹³C NMR (CD₃CN, 125 MHz) δ (ppm): 164.6 (d, J_{C-F} = 6.9 Hz, C_{quat}), 163.3 (dd, ¹J_{C-F} = 255 Hz, ³J_{C-F} = 12.5 Hz, C_{quat}), 162.2 (dd, ¹J_{C-F} = 255 Hz, ³J_{C-F} = 12.5 Hz, C_{quat}), 155.3 (C_{quat}), 154.7 (d, J_{C-F} = 6.6 Hz, C_{quat}), 154.6 (C_{quat}), 151.5 (CH), 150.9 (CH), 149.7 (CH), 148.9 (CH), 143.9 (C_{quat}), 140.4 (CH), 139.1 (CH), 138.8 (CH), 135.5 (CH), 131.6 (C_{quat}), 129.0 (dd, J_{C-F} = 4.6 Hz, J_{C-F} = 2.8 Hz, C_{quat}), 126.6 (CH), 124.9 (t, J = 9.9 Hz, CH), 114.8 (dd, J_{C-F} = 17.8 Hz, J_{C-F} = 3.0 Hz, CH), 99.9 (t, ³J_{C-F} = 27.1 Hz, CH).

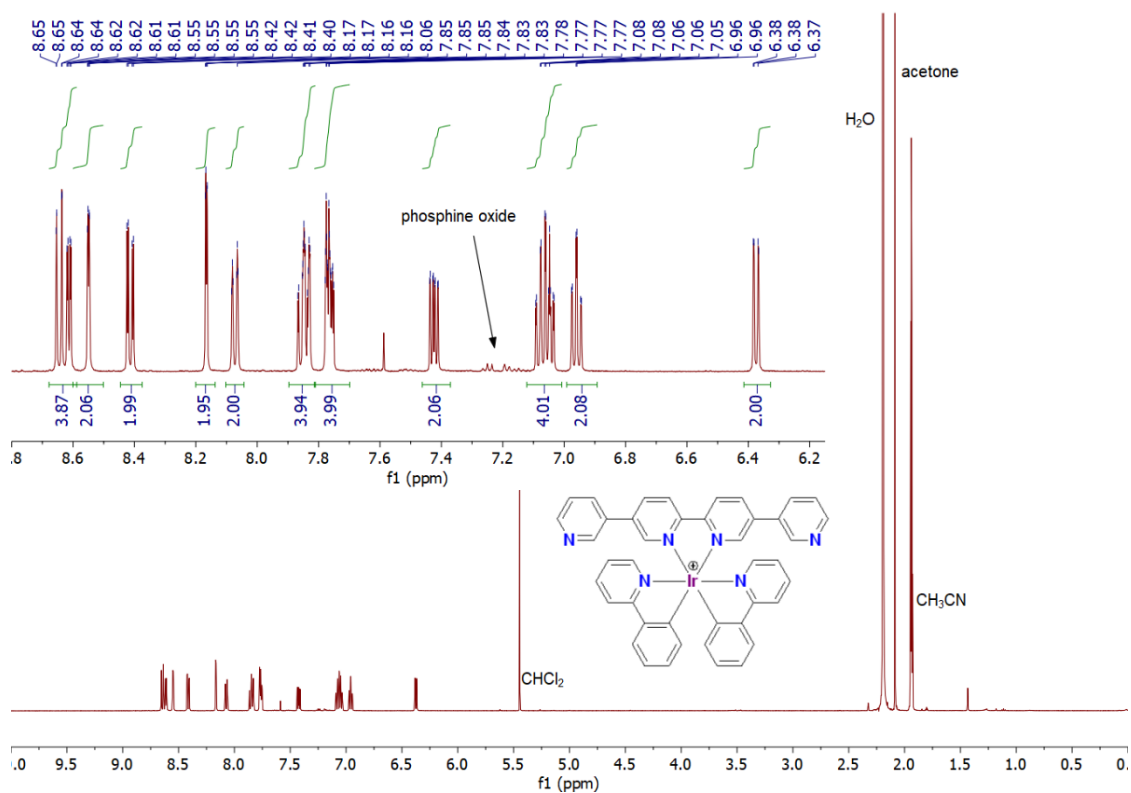
MS (ESI⁺): calcd for [M-PF₆]⁺ C₄₂H₂₆F₄Ir₁N₆ 883.18, found 883.17.

UV-Visible (THF): λ (nm), ε (10³ L.mol⁻¹.cm⁻¹) 290 (40.6), 342 (38.7).

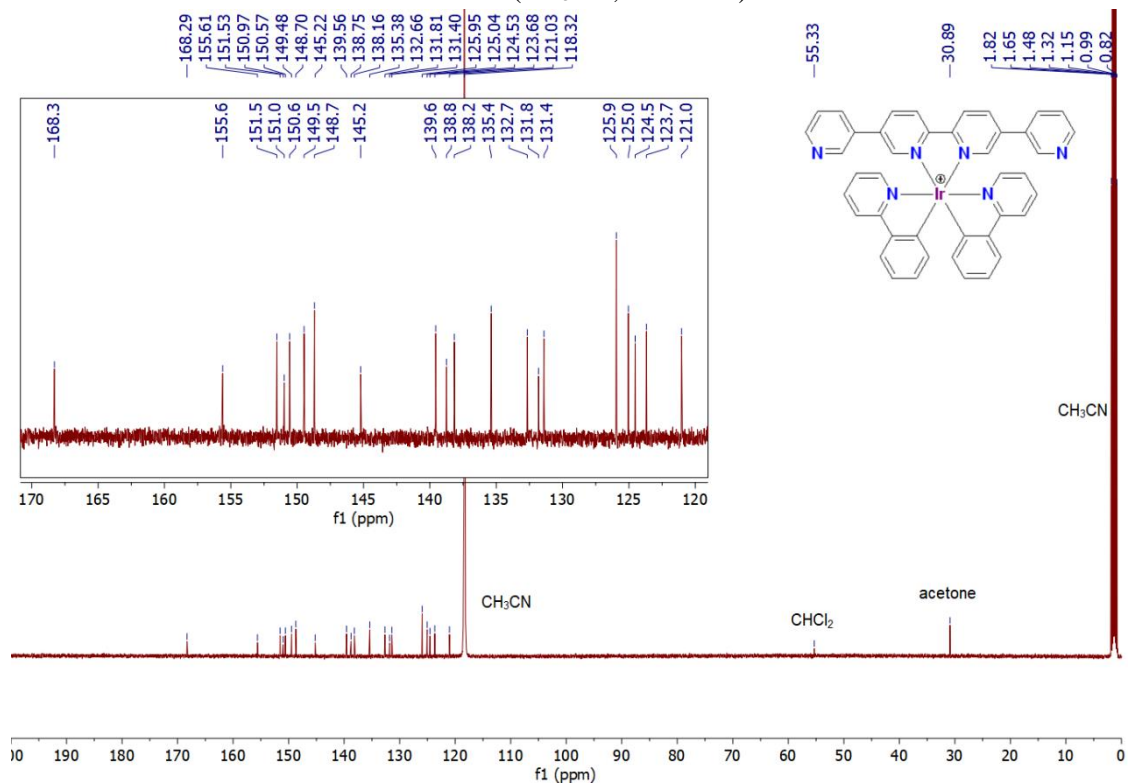
NMR spectra of final complexes

[Ir(ppy)₂(L1)][PF₆]

¹H NMR (CD₃CN, 400 MHz)

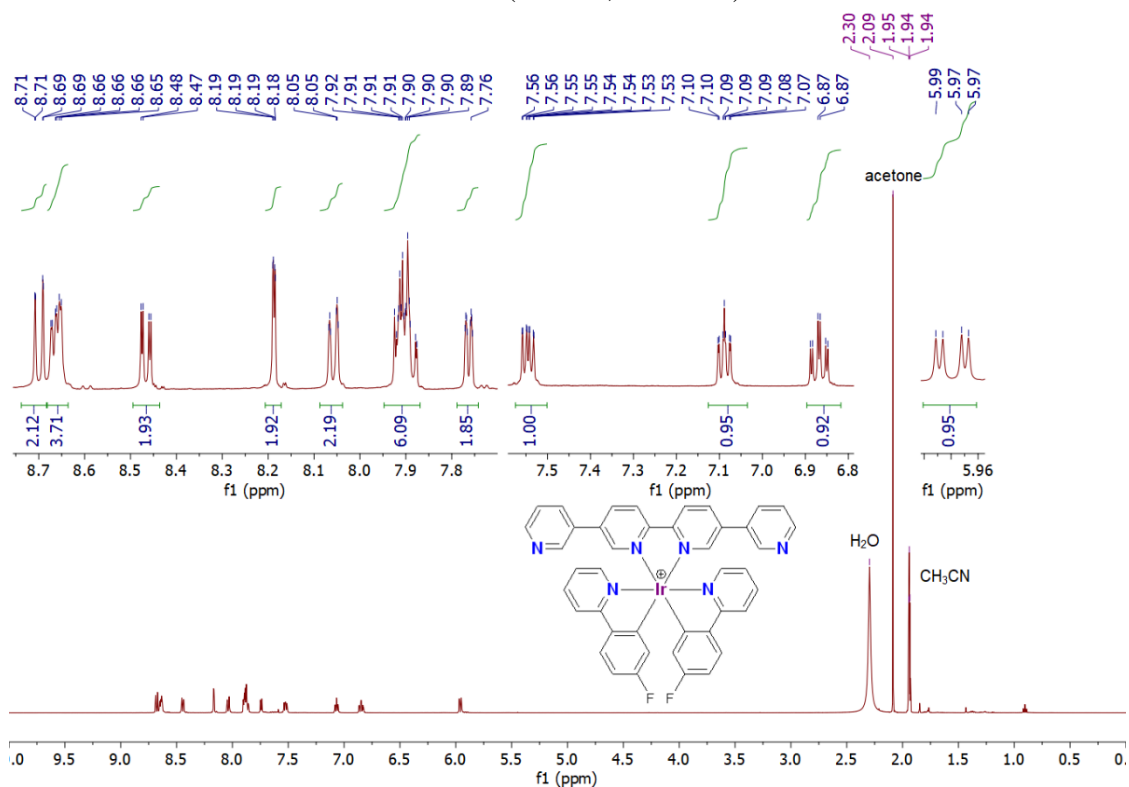


¹³C NMR (CD₃CN, 100 MHz)

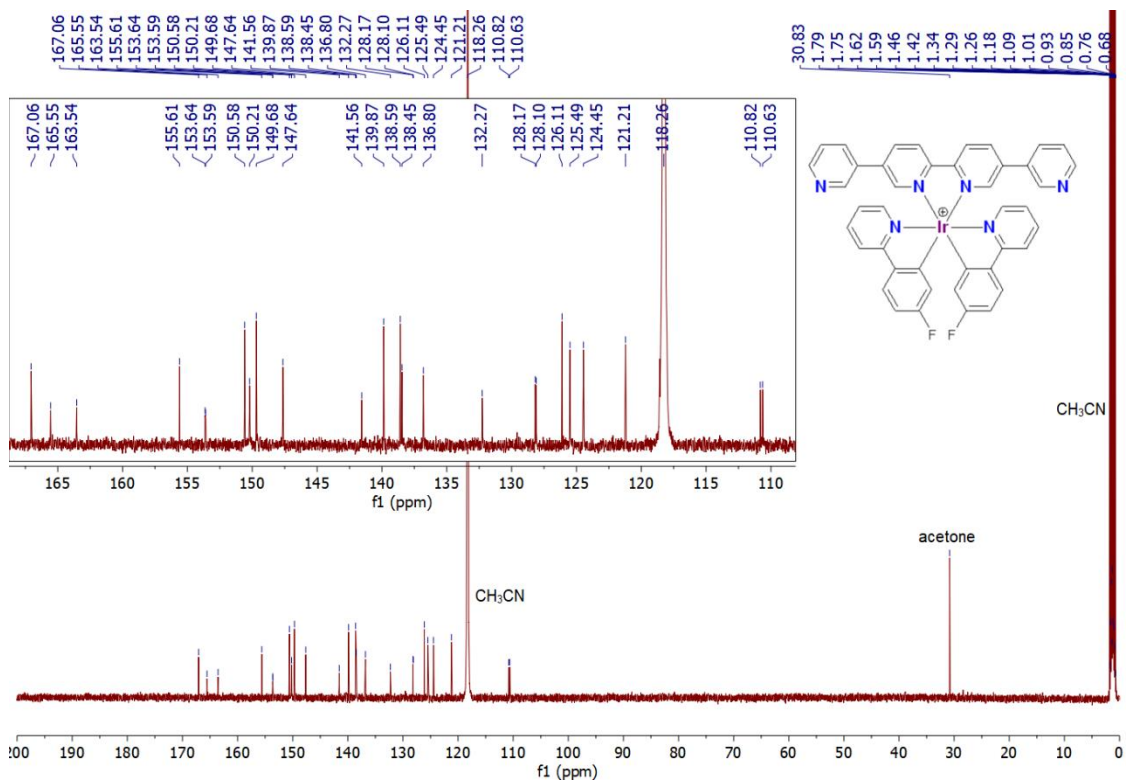


[Ir(Fppy)₂(L1)][PF₆]

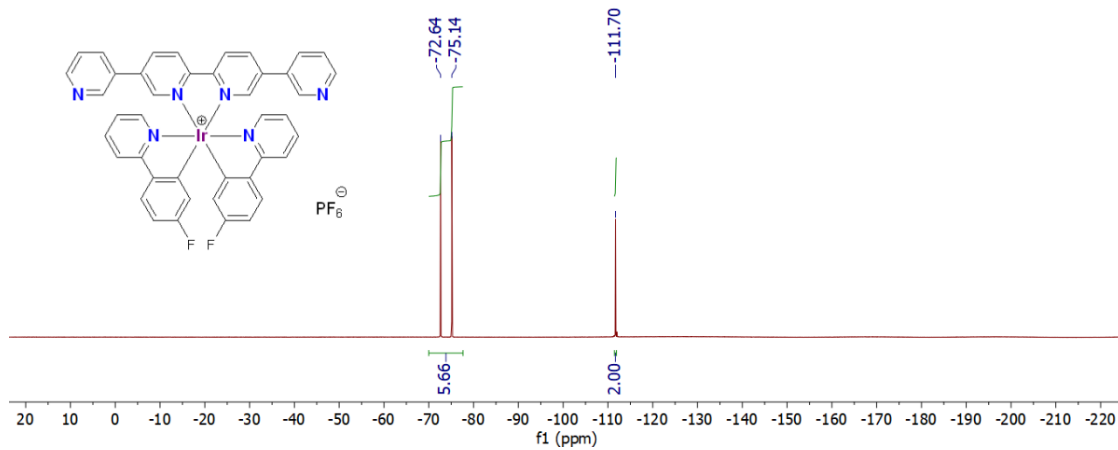
¹H NMR (CD₃CN, 400 MHz)



¹³C NMR (CD₃CN, 100 MHz)

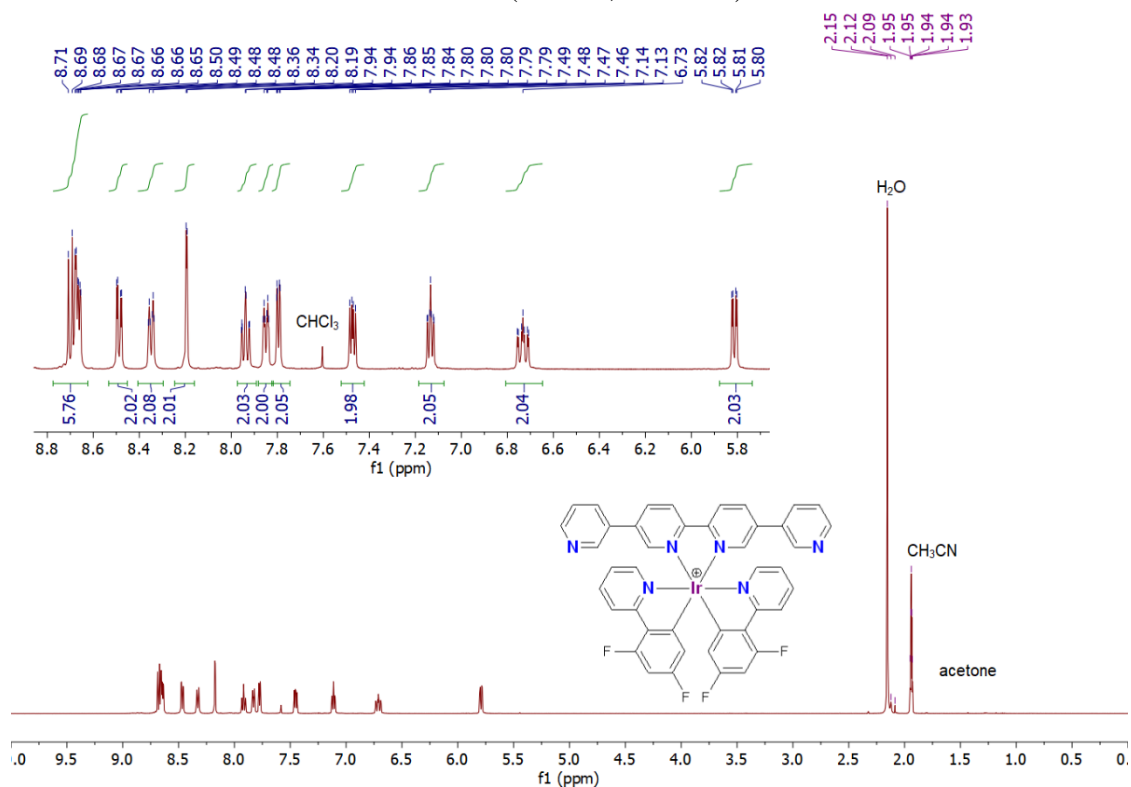


^{19}F NMR (CD_3CN , 282 MHz)

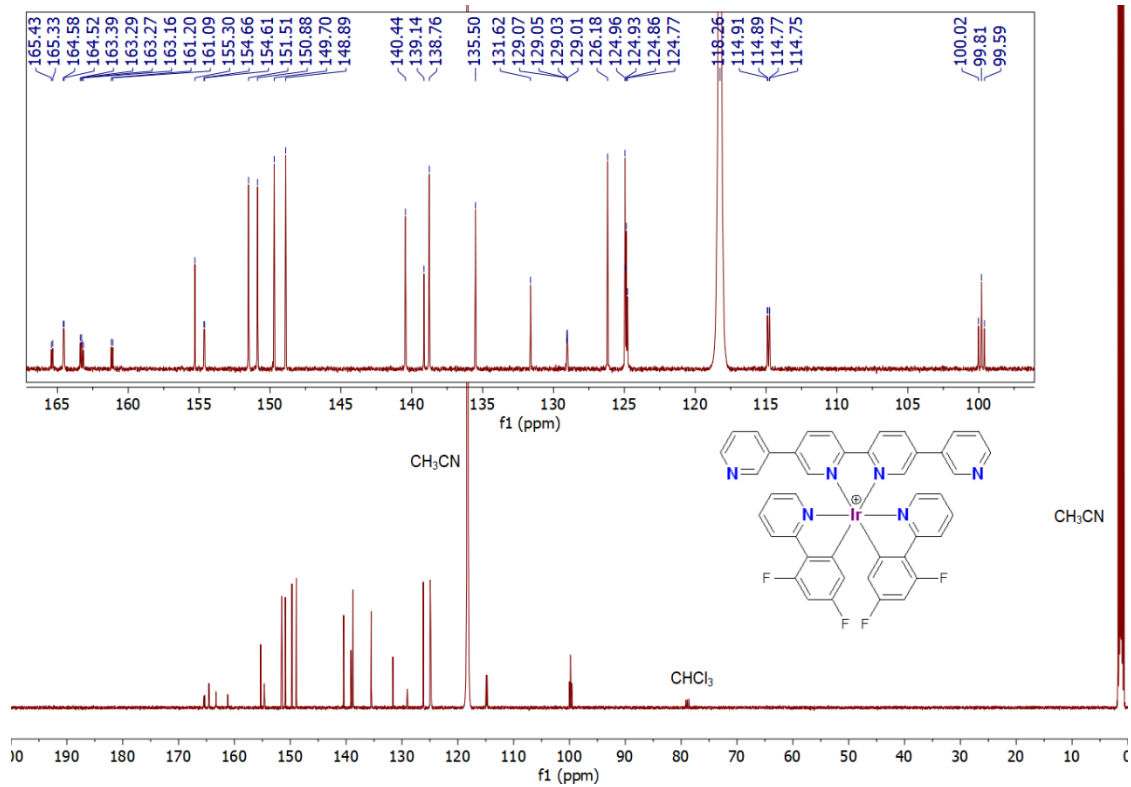


[Ir(dFppy)₂(L1)][PF₆]

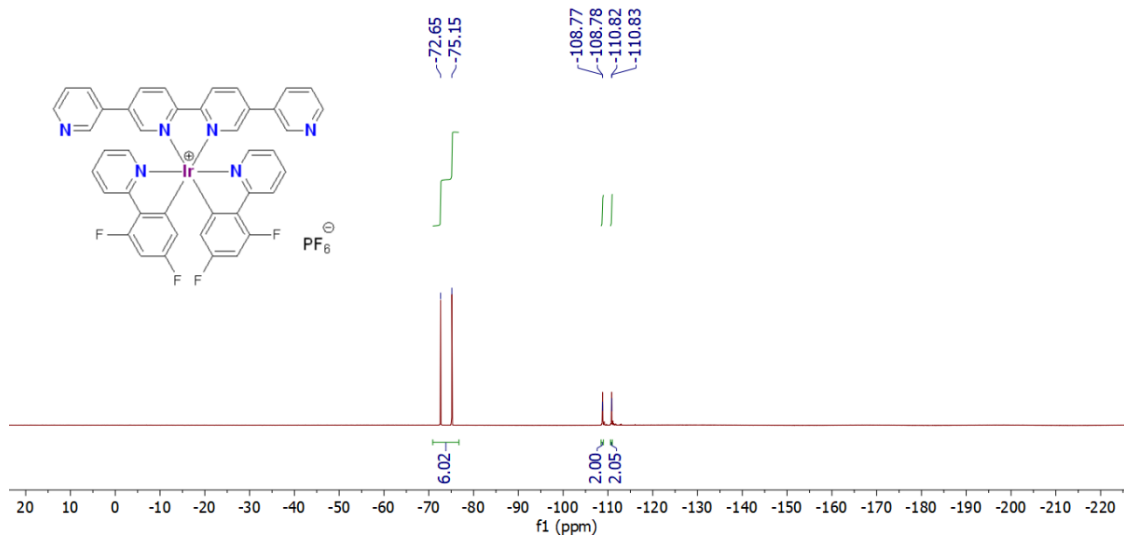
¹H NMR (CD₃CN, 400 MHz)



¹³C NMR (CD₃CN, 125 MHz)

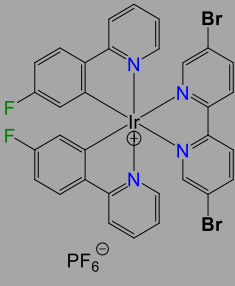
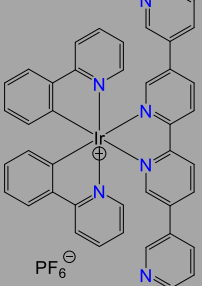
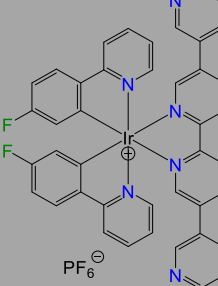
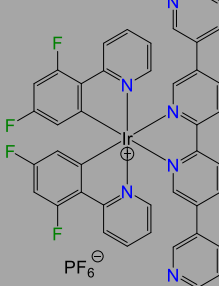


^{19}F NMR (CD_3CN , 282 MHz)



Crystallographic data

Table S1: Crystallographic data for discrete complexes

	 [Ir(Fppy) ₂ (L2)][PF ₆]	 [Ir(ppy) ₂ (L1)][PF ₆]	 [Ir(Fppy) ₂ (L1)][PF ₆]	 [Ir(dFppy) ₂ (L1)][PF ₆]
Formula	C ₃₂ H ₂₀ Br ₂ F ₂ IrN ₄ , PF ₆ , CH ₃ CN	C ₄₂ H ₃₀ IrN ₆ , PF ₆ , 0.7 C ₄ H ₁₀ O (+squeezed solvent)	C ₄₂ H ₂₈ F ₂ IrN ₆ , PF ₆	2(C ₄₂ H ₂₆ F ₄ IrN ₆ , PF ₆), C ₄ H ₁₀ O
FW (g/mol)	1036.56	1007.79	991.87	2129.83
Crystal system	monoclinic	triclinic	triclinic	monoclinic
Space group	P 2 ₁ /c	P-1	P-1	P 2 ₁ /n
<i>a</i> , Å	14.3846(9)	12.3066(3)	10.9258(2)	22.6153(5)
<i>b</i> , Å	9.9896(5)	13.8077(3)	12.5975(3)	11.2357(3)
<i>c</i> , Å	23.4281(13)	14.7006(4)	15.0044(3)	31.8105(8)
<i>α</i> , °	90	80.0580(10)	66.5620(10)	90
<i>β</i> , °	99.105(3)	67.0200(10)	75.1360(10)	93.9120(10)
<i>γ</i> , °	90	67.3610(10)	82.9900(10)	90
<i>V</i> , Å ³	3324.1(3)	2121.84(9)	1830.91(7)	8064.2(3)
<i>Z</i>	4	2	2	4
<i>T</i> , K	173(2)	173(2)	173(2)	173(2)
<i>μ</i> , mm ⁻¹	6.549	3.250	3.773	3.441
Refls. coll.	46738	31800	30087	139161
Ind. Refls. (<i>R</i> _{int})	9513 (0.0586)	9677 (0.0622)	9814 (0.0285)	22267 (0.0639)
<i>R</i> _I (I > 2σ(I)) ^a	0.0387	0.0293	0.0280	0.0435
<i>wR</i> ₂ (I > 2σ(I)) ^a	0.0769	0.0730	0.0675	0.0897
<i>R</i> _I (all data) ^a	0.0677	0.0328	0.0354	0.0681
<i>wR</i> ₂ (all data) ^a	0.0863	0.0749	0.0705	0.0991
<i>GOF</i>	1.022	1.045	1.006	1.054

$$^a R_1 = \sum ||F_0| - |F_c|| / \sum |F_0|; wR_2 = [\sum w(F_0^2 - F_c^2)^2 / \sum wF_0^4]^{1/2}$$

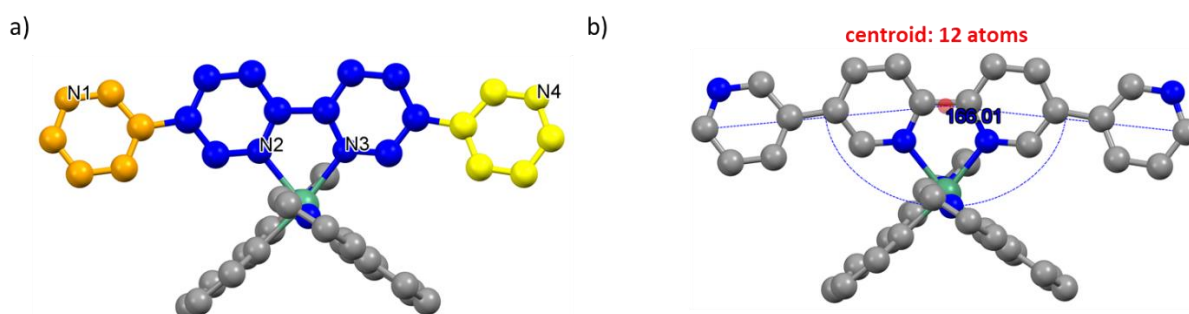
Table S2: Selected bond lengths and angles for [Ir(Fppy)₂(L2)][PF₆] \cdot CH₃CN

[Ir(Fppy) ₂ (L2)][PF ₆] \cdot CH ₃ CN	
Bond lengths	
Ir-N _{L2} (Å)	2.138(4)
	2.152(3)
Ir-N _{ppy} (Å)	2.045(4)
	2.046(4)
Ir-C _{ppy} (Å)	2.016(4)
	2.018(4)
Angles	
N _{L2} -Ir-N _{L2} (°)	76.53(13)
N _{ppy} -Ir-N _{ppy} (°)	172.07(14)
N _{ppy} -Ir-C _{ppy} (°)	80.30(17)
	80.21(17)
Dihedral angles	
bpy N-C-C-N (°)	3.77
Xppy N-C-C-C (°)	-1.91
	-0.64

Table S3 : Selected bond lengths and angles for [Ir(Xppy)₂(L1)][PF₆]

	[Ir(ppy) ₂ (L1)][PF ₆] 0.7C ₄ H ₁₀ O (squeezed)	[Ir(Fppy) ₂ (L1)][PF ₆]	[Ir(dFppy) ₂ (L1)][PF ₆] ·0.5C ₄ H ₁₀ O	
Bond lengths				
Ir-N _{L1} (Å)	2.125(2)	2.131(2)	2.133(3)	2.129(4)
	2.131(3)	2.144(2)	2.152(3)	2.147(3)
Ir-N _{Xppy} (Å)	2.042(3)	2.052(3)	2.043(4)	2.037(3)
	2.058(3)	2.055(3)	2.044(4)	2.040(3)
Ir-C _{Xppy} (Å)	2.003(3)	2.007(3)	2.009(4)	2.006(4)
	2.013(3)	2.008(3)	2.010(4)	2.005(4)
Angles				
N _{L1} -Ir-N _{L1} (°)	76.30(9)	77.02(9)	76.46(13)	76.82(14)
N _{Xppy} -Ir-N _{Xppy} (°)	173.15(10)	172.06(9)	171.39(13)	171.82(14)
N _{Xppy} -Ir-C _{Xppy} (°)	80.27(12)	80.11(11)	80.32(16)	80.70(17)
	80.51(12)	80.45(11)	80.92(18)	80.52(15)
Dihedral angles				
L1 N-C-C-N (°)	-0.79	-2.72	8.91	6.99
	Xppy	-0.14	-1.19	-5.75
N-C-C-C (°)	-3.56	-1.95	-10.49	-10.27
Miscellaneous				
3py-bpy angle (°) ^a	17.78	19.14	2.60	24.24
	21.65	28.34	21.56 / 31.39*	24.88
Curvature angle L1 (°) ^b	166.01	174.45	169.77 / 174.76*	174.20

a) “3py-bpy angle” corresponds to the angle between plane A and plane B as defined in Scheme S1a; b) The “curvature angle **L1**” is defined as highlighted in Scheme S1b; *One of the 3-pyridyl units is disordered over two positions.



Scheme S1: a) Portion of the X-ray structure of [Ir(ppy)₂(L1)][PF₆]
·C₄H₁₀O (squeezed) highlighting the different atoms considered to define plane A and plane B used to measure “3py-bpy angle”. Plane A is the mean plane obtained with the six atoms of the 3-pyridyl units coloured either in yellow or orange while plane B is the mean plane considering the twelve atoms of the bipyridyl unit coloured in blue; b) Portion of the X-ray structure of [Ir(ppy)₂(L1)][PF₆]
·C₄H₁₀O (squeezed) showing the “curvature angle **L1**” defined by the angle between the two carbon atoms in para position with respect to the bpy unit and the centroid of the central bipyridine moiety.

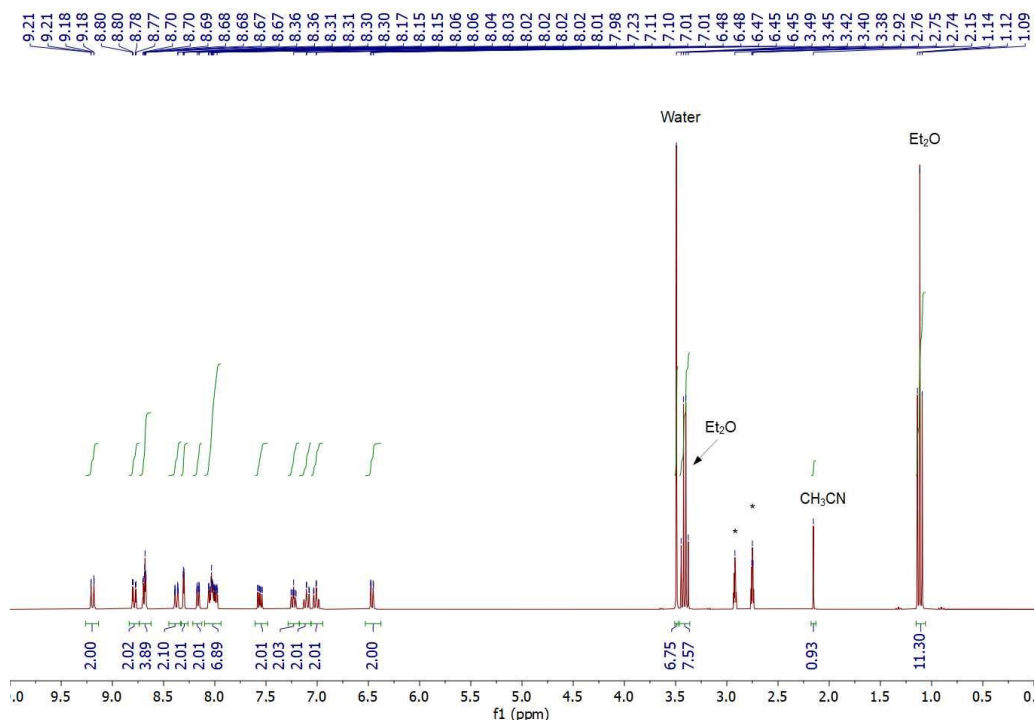


Fig. S1: ^1H NMR spectrum (dmf- d_7 , 300MHz) of single crystals of $[\text{Ir}(\text{ppy})_2(\mathbf{L1})][\text{PF}_6]\cdot\text{C}_4\text{H}_{10}\text{O}$ (squeezed) dissolved in dmf- d_7 highlighting the presence of Et_2O ($\delta = 1.12$ (t) and 3.41 (q) ppm) and CH_3CN ($\delta = 2.15$ ppm, singlet) within the crystal. Water and dmf signals are also present. Those crystals were used to solve the crystal structure by X-Ray diffraction. Integration of signals shows the presence of one CH_3CN molecule and almost two Et_2O molecules per one Ir complex molecule. Because Et_2O was used as solvent to wash the red crystals, integration of its signal is most probably overestimated. The X-Ray study revealed the presence of residual densities corresponding to 34 electrons that could not be assigned with certainty, and it was thus squeezed. According to the NMR spectrum above, this density might be attributed to CH_3CN molecules.

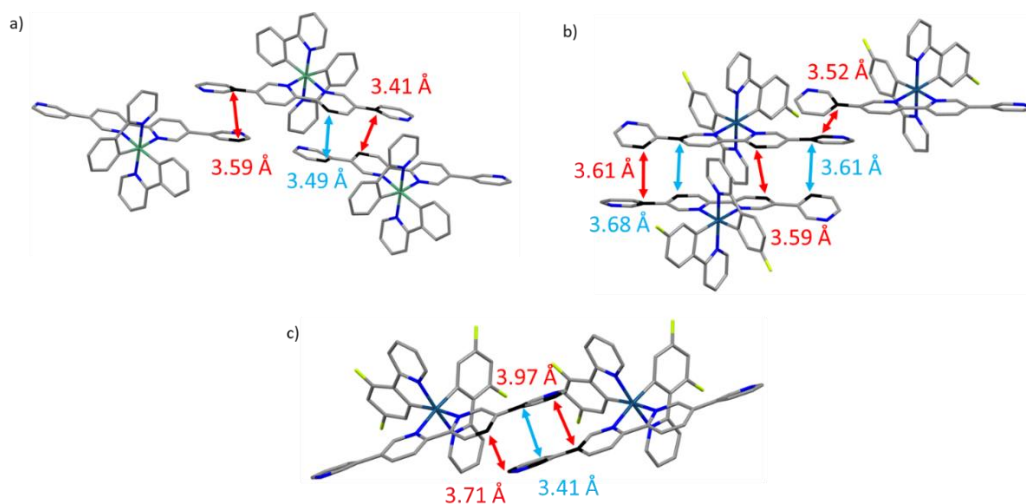


Fig. S2: Portions of the X-ray structure of $[\text{Ir}(\text{ppy})_2(\mathbf{L1})][\text{PF}_6]\cdot\text{C}_4\text{H}_{10}\text{O}$ (squeezed) (a), $[\text{Ir}(\text{Fppy})_2(\mathbf{L1})][\text{PF}_6]$ (b) and $[\text{Ir}(\text{dFppy})_2(\mathbf{L1})][\text{PF}_6]\cdot\text{C}_4\text{H}_{10}\text{O}$ (c) showing π - π interactions between two complexes in the crystal packing. The distances reported correspond to C-C distances, with the C atoms considered depicted in black. H atoms, PF_6 anions and solvent molecules have been omitted for clarity.

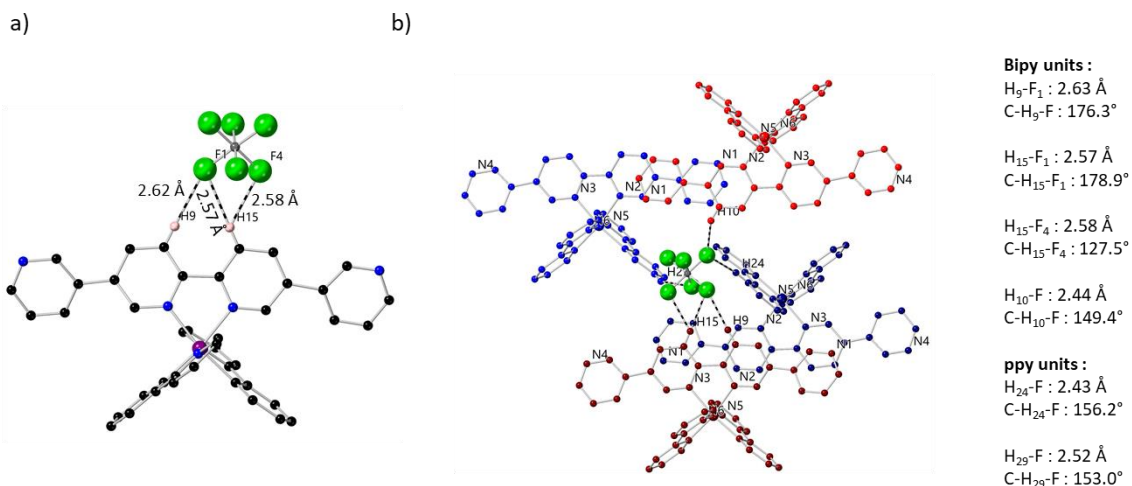


Fig. S3: Portions of the X-ray structure of $[Ir(ppy)_2(L1)][PF_6] \cdot C_4H_{10}O$ (squeezed) showing non classical hydrogen bonds of the PF_6 anion and five distinct Ir complexes in the crystal packing. The distances reported correspond to H-F distances. Only the H atoms involved in H-bonding are represented. Other H atoms and PF_6 anions have been omitted for clarity. Electron density related to some solvent molecules was removed using the SQUEEZE command because of a severe disorder. Et_2O solvent molecules are not represented in the figure.

A rather short H-F distance is observed between two H atoms belonging to one bpy moiety, acting as a chelating unit, and two fluorine atoms belonging to one PF_6 anion (H-F distance of 2.58 to 2.63 Å, C-H-F angles *ca.* 177° and 127.5°, Fig. S3a). This Ir complex is depicted in dark red on Fig. S3b. Such interactions have been reported before.⁹ It should be noted that, contrary to what was observed for similar cationic Ir complexes having Cl as counterion,^{10,11} only one bipyridine unit is involved as a chelating moiety. The other bipyridine unit belonging to a second Ir complex (depicted in red, Fig. S3b) display only one $F \cdots HC$ interaction between one H atom located on position 4 of the bpy unit and another F atom of the anion (H-F distance of 2.44 Å, C-H-F angles 149.4°).

Finally, the same PF_6 anion exhibits close contacts with H atoms located on the phenyl units (light blue) and on the pyridyl moieties (dark blue and blue) of two distinct ppy moieties belonging to two other Ir complexes ($H_{Ph}-F$ distance of 2.43 Å and $H_{Py}-F$ distances of 2.52 Å, C-H-F angles 156.2° and 153.0° respectively) (Fig. S3b).

A short H-F distance is also observed between one F atom of the PF_6 anion and one Et_2O molecule (H-F distance of 2.54 Å, C-H-F angle 146.96°) (not represented on FigS3b for clarity).

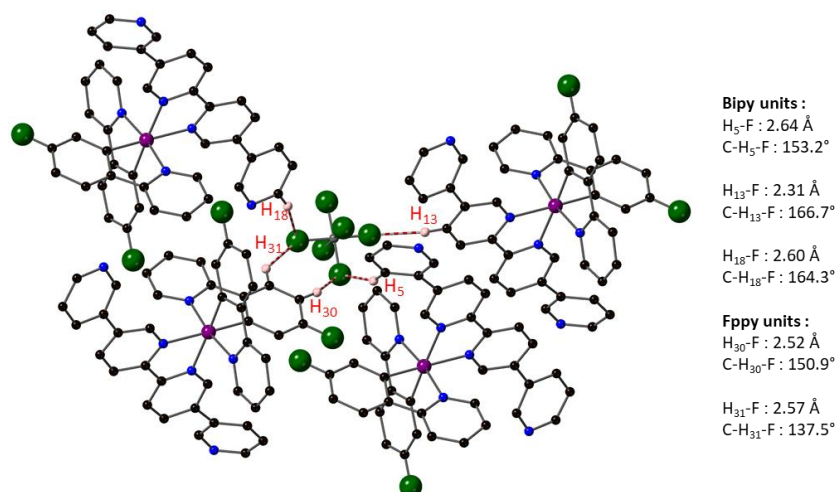


Fig. S4: Portions of the X-ray structure of $[\text{Ir}(\text{Fppy})_2(\text{L1})][\text{PF}_6]$ showing non-classical hydrogen bonds of the PF_6 anion and four distinct Ir complexes in the crystal packing. The distances reported correspond to H-F distances. Only the H atoms involved in H-bonding are represented. Other H atoms and PF_6 anions have been omitted for clarity.

A rather short distance of 2.31 Å is observed between one F atom of the anion and one H atom located on position 4 of the bpy moiety (C-H-F angle of 166.7°). The two H atoms of the phenyl unit belonging to one Fppy ligand exhibit H-F distances of 2.52 and 2.57 Å (C-H-C angles of 150.9 and 137.5° respectively). The third and fourth Ir complexes involved in the H-bond pattern are connected to the PF_6 anion through one H atom located either in position 4 or 6 of the 3-pyridyl terminal group belonging to **L1** with longer H-F distances of 2.60 and 2.64 Å respectively (C-H-C angles of 164.3 and 153.2° respectively).

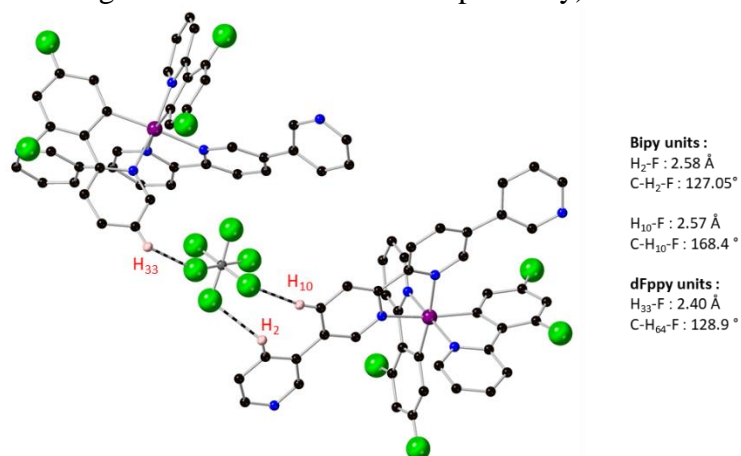


Fig. S5: Portions of the X-ray structure of $[\text{Ir}(\text{dFppy})_2(\text{L1})][\text{PF}_6] \cdot \text{C}_4\text{H}_{10}\text{O}$ showing non-classical hydrogen bonds of the PF_6 anion and two distinct Ir complexes in the crystal packing. The distances reported correspond to H-F distances. Only the H atoms involved in H-bonding are represented. Other H atoms, PF_6 anions and Et_2O molecules have been omitted for clarity. Disorder on one of the peripheral 3-pyridyl units has not been represented for clarity.

Two of the H-F interactions involve two F atoms of one PF_6 ion and one H atom located on position 4 of the bpy backbone (H-F distance 2.57 Å, C-H-F angle 168.4°) and one H atom located on position 2 of the 3-pyridyl terminal group of the same bpy ligand (H-F distance 2.58 Å, C-H-F angle 127.0°). The third interaction involves a second Ir complex for which one H atom located on position 5 of the pyridyl unit belonging to a dFppy ligand display short contact with a third F atom of the PF_6 anion (H-F distance 2.40 Å, C-H-F angle 128.9°).

Table S4 : Crystallographic data for coordination polymers

	CP1_{Br}	CP2_{Cl}	CP2_{Br}	CP2_I	CP3_{Cl}	CP3_{Br}	CP3_I^a
Metallatecton	[Ir(ppy) ₂ (L1)] ⁺	[Ir(Fppy) ₂ (L1)] ⁺			[Ir(dFppy) ₂ (L1)] ⁺		
Metallic salt	CdBr ₂	CdCl ₂	CdBr ₂	CdI ₂	CdCl ₂	CdBr ₂	CdI ₂
Formula	C ₈₄ H ₆₀ Br _{7.28} Cd ₃ Cl _{0.72} Ir ₂ N ₁₂ , 2 CHCl ₃	C ₈₄ H ₅₆ Cd ₃ Cl ₈ F ₄ Ir ₂ N ₁₂ , 1.7CHCl ₃ + solvent	C ₈₄ H ₅₆ Br _{6.78} Cd ₃ Cl _{1.22} F ₄ Ir ₂ N ₁₂ , 1.7 CHCl ₃	C ₄₂ H ₂₈ Cd _{1.46} Cl _{1.94} F ₂ I _{2.45} Ir N ₆ , CHCl ₃	C ₈₄ H ₅₂ Cd ₃ Cl ₈ F ₈ Ir ₂ N ₁₂ , + solvent	C ₈₄ H ₅₂ Br ₈ Cd ₃ F ₈ Ir ₂ N ₁₂ , + solvent	C ₈₄ H ₅₂ Cd ₃ Cl ₂ F ₈ I ₆ Ir ₂ N ₁₂ , 1.202 CHCl ₃
FW(g/mol)	2805.04	2517.53	2818.97	1510.05	2386.57	2742.25	3078.82
Crystal system	Triclinic	Triclinic	Triclinic	Triclinic	Triclinic	Triclinic	Triclinic
Space group	P -1	P-1	P-1	P-1	P -1	P -1	P -1
<i>a</i> , Å	9.6808(5)	9.5750(3)	9.6452(6)	9.7057(2)	9.6716(3)	9.7282(3)	9.7207(3)
<i>b</i> , Å	14.3456(7)	14.2134(4)	14.3456(8)	14.5895(4)	13.8319(4)	14.2740(5)	14.6181(5)
<i>c</i> , Å	17.4662(8)	17.6636(5)	17.6310(11)	17.6961(4)	17.6708(5)	17.6802(6)	17.6742(6)
α , °	92.283(2)	91.8870(10)	91.978(2)	91.3200(10)	92.935(2)	92.379(2)	91.285(2)
β , °	105.186(2)	105.5820(10)	105.268(2)	105.8290(10)	102.647(2)	103.849(2)	105.818(2)
γ , °	106.412(2)	106.2460(10)	106.498(2)	106.9280(10)	106.392(2)	106.806(2)	106.908(2)
<i>V</i> , Å ³	2228.52(19)	2207.85(11)	2240.7(2)	2291.98(10)	2196.65(12)	2265.65(13)	2297.76(14)
<i>Z</i>	1	1	1	2	1	1	1
<i>T</i> , K	173(2)	173(2)	173(2)	173(2)	173(2)	173(2)	173(2)
μ , mm ⁻¹	7.430	4.171	6.930	5.557	4.043	7.211	5.815
Refls. coll.	32847	98748	19494	17100	88882	100525	29673
Ind. Refls. (<i>R</i> _{int})	10746 (0.0496)	11895 (0.0306)	9652 (0.0326)	8629 (0.0293)	11743 (0.0369)	12468 (0.0429)	11765 (0.0446)
<i>R</i> _I (<i>I</i> > 2 σ (<i>I</i>)) ^a	0.0416	0.0356	0.0397	0.0367	0.0397	0.0369	0.0631
<i>wR</i> ₂ (<i>I</i> > 2 σ (<i>I</i>)) ^a	0.1013	0.0900	0.0947	0.0868	0.0975	0.0838	0.1818
<i>R</i> _I (all data) ^a	0.0600	0.0442	0.0544	0.0483	0.0582	0.0587	0.0838
<i>wR</i> ₂ (all data) ^a	0.1093	0.0956	0.1022	0.0933	0.1095	0.0918	0.1997
<i>GOF</i>	1.042	1.028	1.032	1.019	1.035	1.022	1.005

^aBecause of the poor quality of crystal data for **CP3_I**, the cif file was not deposited in the CCDC. The data reported here are the result of a preliminary refinement of the crystal data which shows the formation of the Cd₃X₈ node similar to the crystal structure of **CP2_I** as depicted in the figures provided below

Table S5 : Selected bond lengths and angles for the coordination polymers

	CP1 _{Br}	CP2 _{Cl}	CP2 _{Br}	CP2 _I	CP3 _{Cl}	CP3 _{Br}	CP3 _I
Metallatecton	[Ir(ppy) ₂ (L1)] ⁺	[Ir(Fppy) ₂ (L1)] ⁺			[Ir(dFppy) ₂ (L1)] ⁺		
CdX ₂	CdBr ₂ ^g	CdCl ₂	CdBr ₂	CdI ₂ ^g	CdCl ₂	CdBr ₂	CdI ₂
Bond lengths (Å)							
Ir-N _{Xppy} ^a	2.038	2.040	2.036	2.053	2.036	2.046	2.032
Ir-C _{Xppy} ^a	2.032	2.032	2.028	2.022	2.000	2.011	2.010
Ir-N _{L1}	2.128(4); 2.138(4)	2.132(3); 2.115(3)	2.132(5); 2.111(5)	2.125(5); 2.115(5)	2.118(4); 2.124(4)	2.120(3); 2.126(4)	2.111(6); 2.121(7)
Cd _{ext} -N	2.420(5)	2.408(4)	2.418(5)	2.454(6)	2.401(4)	2.418(4)	2.450(7)
Cd _{int} -N	2.356(4)	2.348(3)	2.354(5)	2.356(5)	2.357(4)	2.363(3)	2.347(7)
Cd _{ext} -X	2.43(3)/2.6064(11); 2.6063(7)	2.5001(11); 2.5028(12)	2.55(4)/2.608(2); 2.600(8)	2.31(2)/2.7773(8) 2.7733(7)	2.477(14); 2.4801(16)	2.5954(6); 2.5994(6)	2.679 (I); 2.761(I) ^f
Cd _{ext} -(μ-X)	2.560(16)/2.7929(19); 2.7554(7)	2.6315(10); 2.6144(10)	2.552(10)/2.797(3); 2.7449(8)	2.7301(17); 2.764(12)/2.909(4)	2.6095(13); 2.6393(12)	2.7432(5); 2.7984(6)	2.743(2) (Cl); 2.8968 (9) (I)
Cd _{int} -(μ-X)	2.67(2)/ 2.633(3); 2.8423(6)	2.5444(9); 2.7050(10)	2.649(13)/2.611(15); 2.8351(6)	2.5574(15); 2.776(9)/3.013(3)	2.5375(12); 2.6971(11)	2.6457(4); 2.8475(5)	2.5631(19) (Cl); 2.9899(7) (I)
Angles (°)							
N _{Xppy} -Ir-N _{Xppy}	177.5(4); 168.9(3)	179.5(3); 168.1(3)	178.1(5); 166.2(4)	177.3(10); 167.2(11)	178.7(4); 168.5(3)	179.1(4); 168.0(3)	169.8(6); 177.6(4)
N _{L1} -Ir-N _{L1}	76.53(16)	76.63 (13)	76.57(18)	76.91(19)	76.85(15)	76.73(14)	76.7(2)
N _{Xppy} -Ir-C _{Xppy} ^b	80.8	80.2	80.1	81.1	80.2	79.7	80.8
N-Cd _{int} -N	180.00(12)	180.0	180.00(19)	180.0	180.0	180.0	180.0(3)
N-Cd _{int} -(μ-X)	88.4(4)/89.08(12); 91.6(4)/90.92(12); 91.00(12); 89.00(12)	88.74(9); 91.00(9); 91.26(9); 89.00(9)	88.144/88.399; 91.856/91.600; 88.934; 91.066	91.86(14); 88.14(14); 89.2(3)/89.23(18); 90.8(3)/90.77(18)	88.85(10); 89.32(10); 90.68(10); 91.15(10)	88.74(10); 89.45(9); 90.55(9); 91.27(10)	87.85(19) (Cl); 92.15(19) (Cl); 89.3(2) (I); 90.7(2) (I)
N-Cd _{ext} -(μ-X)	85.76(12); 162.4(5)/164.43(13)	85.59(9); 163.98(9)	85.69(13); 161.8(3)/164.543	89.5(2)/84.74(15); 165.58(14)	85.10(11); 164.82(12)	85.51(19); 164.95(10)	86.50(18) (I); 165.6(2) (Cl)
N-Cd _{ext} -X	85.2(8)/90.87(11); 93.67(12)	90.09(10); 93.17(10)	89.0(9)/90.921; 94.07(13)	108.4(7)/92.75(14); 92.10(14)	90.90(11); 92.92(13)	91.57(9); 93.75(10)	91.9; 94.8 ^f
Miscellaneous							
Cd _{int} -Cd _{int} (Å)	20.584	20.407	20.512	20.609	20.359	20.535	20.648
3py-bpy angle (°) ^c	35.8; 48.0	35.5; 47.4	35.5; 47.8	34.1; 47.7	34.5; 46.8	35.5; 48.4	34.0; 47.1
Curvature angle L1 (°) ^d	170.89	170.88	170.53	169.67	171.39	171.14	169.51
d _{CP-CP} (Å) ^e	17.47	17.69	17.63	17.71	17.67	17.68	17.67
d _{planes} (Å) ^e	9.68	9.58	9.65	9.71	9.67	9.73	9.72

a) Because of the disorder observed on the positions of the Xppy ligands (statistical presence of Δ and Λ enantiomers), only average Ir-C_{Xppy} and Ir-N_{Xppy} bond lengths are given; b) The angles given correspond to an average N-Ir-C angle for the N and C atoms belonging to the same Xppy unit; c) The “3py-bpy angle” is defined as highlighted in Scheme S1a; d) The “curvature angle L1” is defined as highlighted in Scheme S1b; e) distance between two Cd atoms Cd_{int}-Cd_{int} of two parallel coordination polymers, d_{CP-CP}, or two distinct planes d_{planes} (see Fig. 5); f) Because the monodentate I⁻ ligand is disordered over two positions, only average Cd_{ext}-I bond lengths and N-Cd_{ext}-X angles are given; g) Distances and angles containing Cl atoms are highlighted in green while they are written in black for Br or I.

Table S6 : Site occupancy for the Xppy ligands in the coordination polymers^a

	CP1_{Br}	CP2_{Cl}	CP2_{Br}	CP2_I	CP3_{Cl}	CP3_{Br}	CP3_I
Metallatecton	[Ir(ppy) ₂ (L1)] ⁺	[Ir(Fppy) ₂ (L1)] ⁺	[Ir(Fppy) ₂ (L1)] ⁺	[Ir(Fppy) ₂ (L1)] ⁺	[Ir(dFppy) ₂ (L1)] ⁺	[Ir(dFppy) ₂ (L1)] ⁺	[Ir(dFppy) ₂ (L1)] ⁺
CdX ₂	CdBr ₂	CdCl ₂	CdBr ₂	CdI ₂	CdCl ₂	CdBr ₂	CdI ₂
Enantiomer 1	45.0	49.2	45.0	46.0	43.6	47.1	39.9
Enantiomer 2	55.0	50.8	55.0	54.0	56.4	52.9	60.1

^aRelative ratio of one enantiomer over the other one considering only one complex.

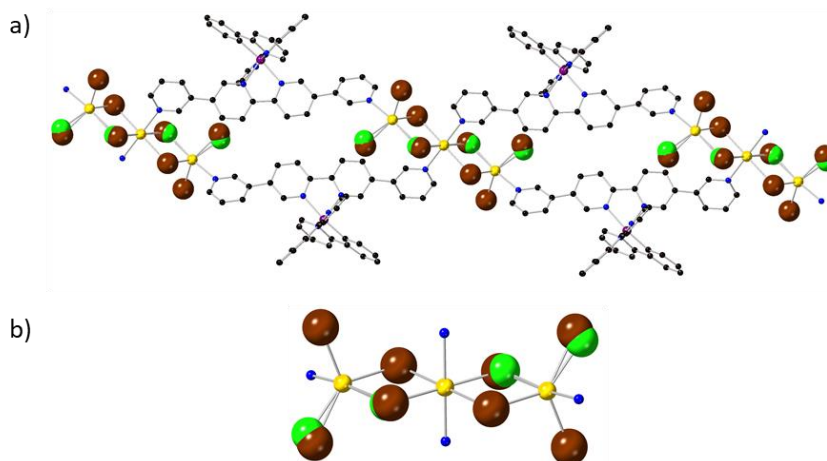


Fig. S6: Portions of the X-Ray structures of **CP1_{Br}** (a) showing the formation of infinite 1D coordination polymers thanks to the assembly of the cationic metallatecton $[\text{Ir}(\text{ppy})_2(\mathbf{L1})]^+$ and the trinuclear metallic nodes $[\text{Cd}_3\text{Cl}_n\text{Br}_{(8-n)}]^{2-}$ ($n=0$ to 4) represented alongside the respective CP (b) illustrating its behaviour as a 4-four distorted square planar connecting node and showing the mixture of Cl/Br atoms found at some positions of the Cd node. For the sake of clarity, only one enantiomer of the Ir complexes has been arbitrary represented even though a statistical distribution of Δ and Λ isomers is observed. H atoms and chloroform solvent molecules have been omitted.

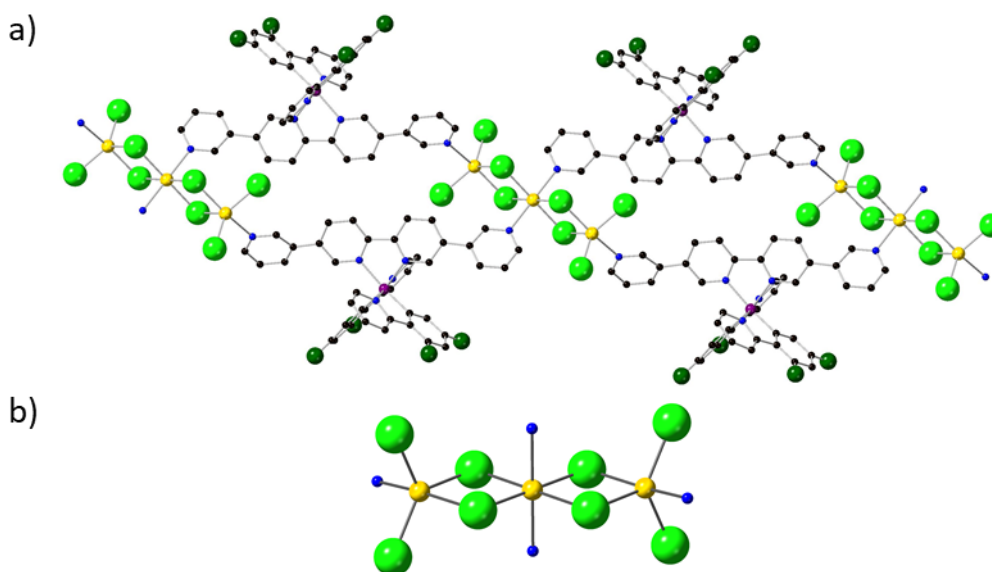


Fig. S7: Portions of the X-Ray structures of **CP3_{Cl}** (a) showing the formation of infinite 1D coordination polymers thanks to the assembly of the cationic metallatecton $[\text{Ir}(\text{dFppy})_2(\mathbf{L1})]^+$ and the trinuclear metallic nodes $[\text{Cd}_3\text{Cl}_8]^{2-}$ represented alongside the respective CP (b) illustrating its behaviour as a 4-four distorted square planar connecting node. For the sake of clarity, only one enantiomer of the Ir complexes has been arbitrary represented even though a statistical distribution of Δ and Λ isomers is observed. H atoms and chloroform solvent molecules have been omitted.

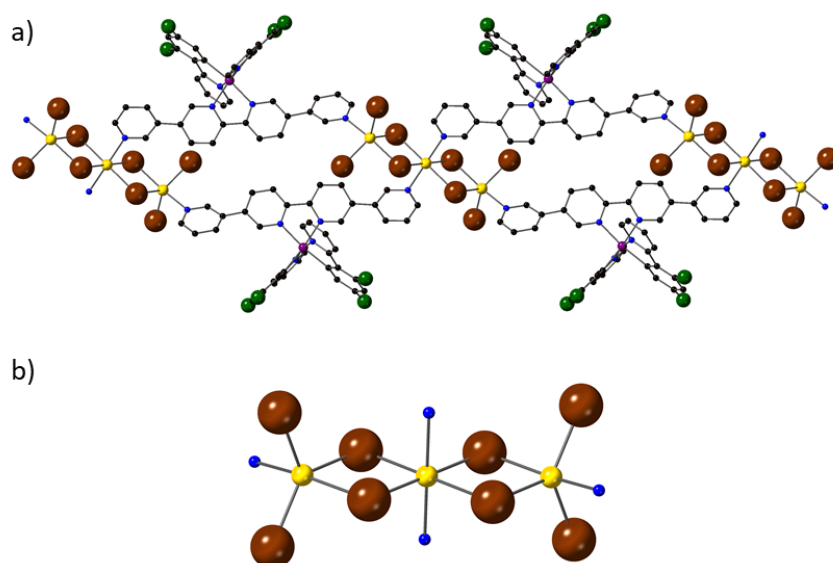


Fig. S8: Portions of the X-Ray structures of **CP3_{Br}** (a) showing the formation of infinite 1D coordination polymers thanks to the assembly of the cationic metallatecton $[\text{Ir}(\text{dFppy})_2(\mathbf{L1})]^+$ and the trinuclear metallic nodes $[\text{Cd}_3\text{Br}_8]^{2-}$ represented alongside the respective CP (b) illustrating its behaviour as a 4-4 distorted square planar connecting node. For the sake of clarity, only one enantiomer of the Ir complexes has been arbitrary represented even though a statistical distribution of Δ and Λ isomers is observed. H atoms and chloroform solvent molecules have been omitted. Presence of a mixture of Cl atoms and Br atoms in the trinuclear Cd node is possible as in the case of **CP1_{Br}** but this has not been modelled.

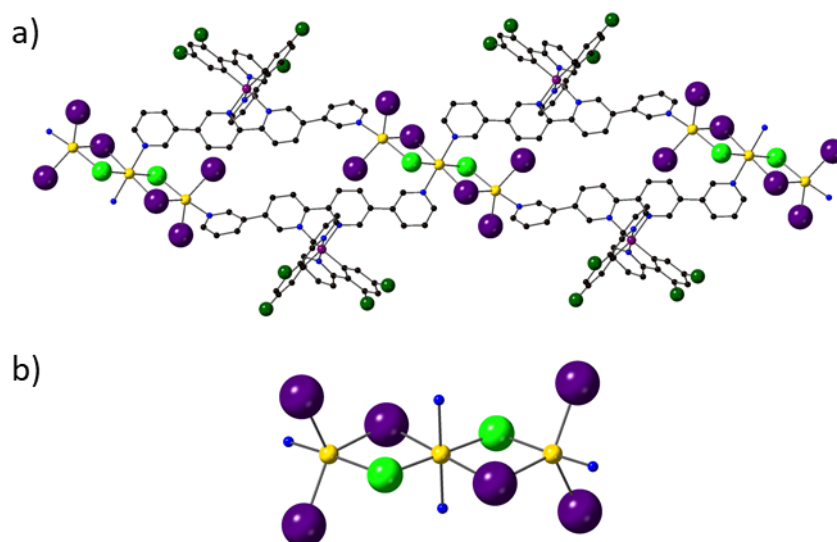


Fig. S9: Portions of the X-Ray structures of **CP3_I** (a) showing the formation of infinite 1D coordination polymers thanks to the assembly of the cationic metallatecton $[\text{Ir}(\text{dFppy})_2(\mathbf{L1})]^+$ and the trinuclear metallic nodes $[\text{Cd}_3\text{I}_6\text{Cl}_2]^{2-}$ represented alongside the respective CP (b) illustrating its behaviour as a 4-4 distorted square planar connecting node. For the sake of clarity, only one enantiomer of the Ir complexes has been arbitrary represented even though a statistical distribution of Δ and Λ isomers is observed. The two monodentate iodide ligands are disordered over two positions but for clarity reasons, only one position is represented. H atoms and chloroform solvent molecules have been omitted.

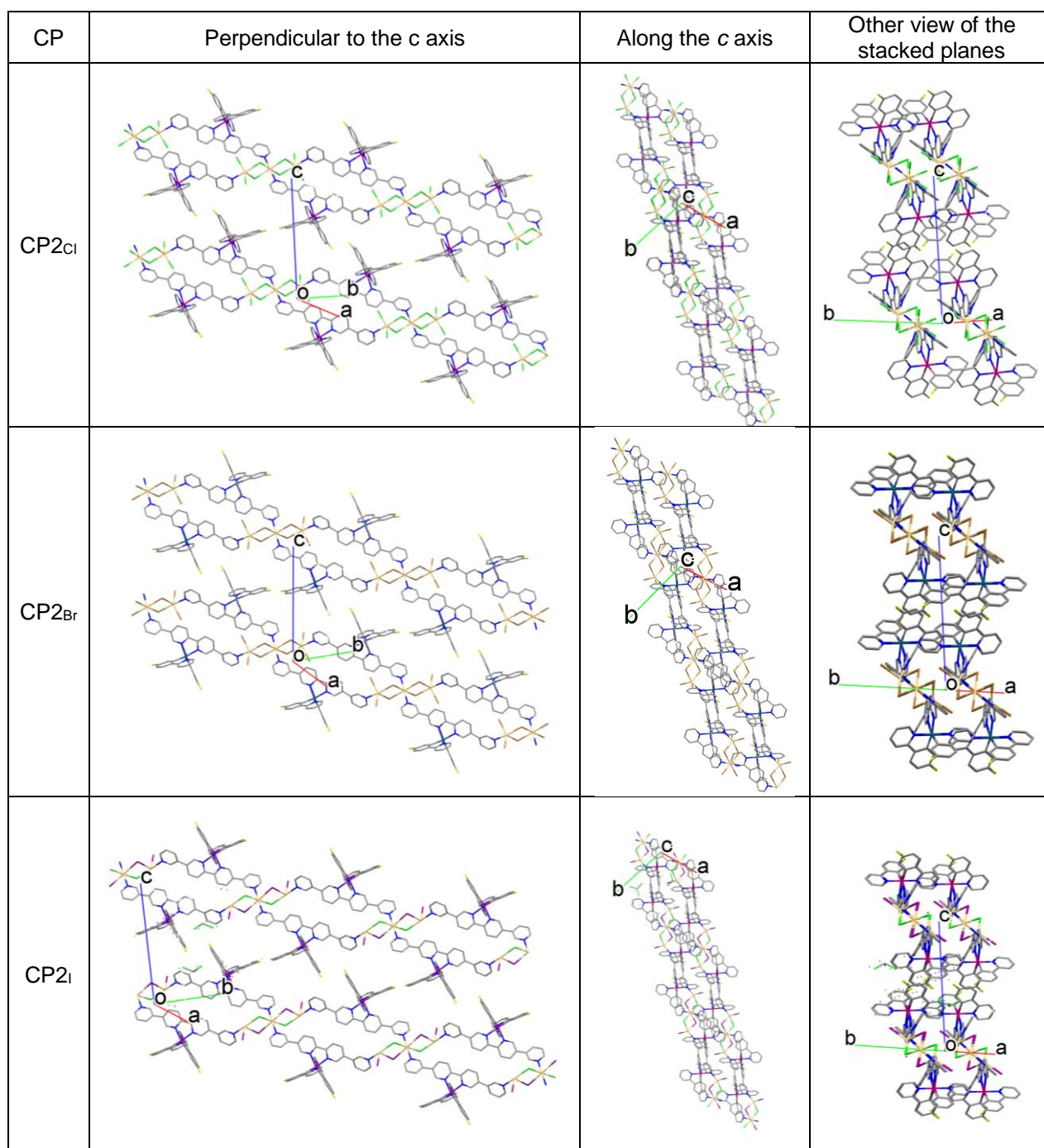


Fig. S10: Portions of the X-Ray structures of **CP2_x** showing the formation of one plane made of parallel 1D coordination polymers represented perpendicular to the *c* axis (a) and stacking of consecutive planes along two distinct directions. For the sake of clarity, only one enantiomer of the Ir complexes has been arbitrary represented even though a statistical distribution of Δ and Λ isomers is observed. For **CP2_{Br}** and **CP2_I**, in case of a mixture of Br/I atoms with Cl atoms, only Br/I atoms have been represented and Cl atoms have been omitted within the Cd trinuclear node for clarity

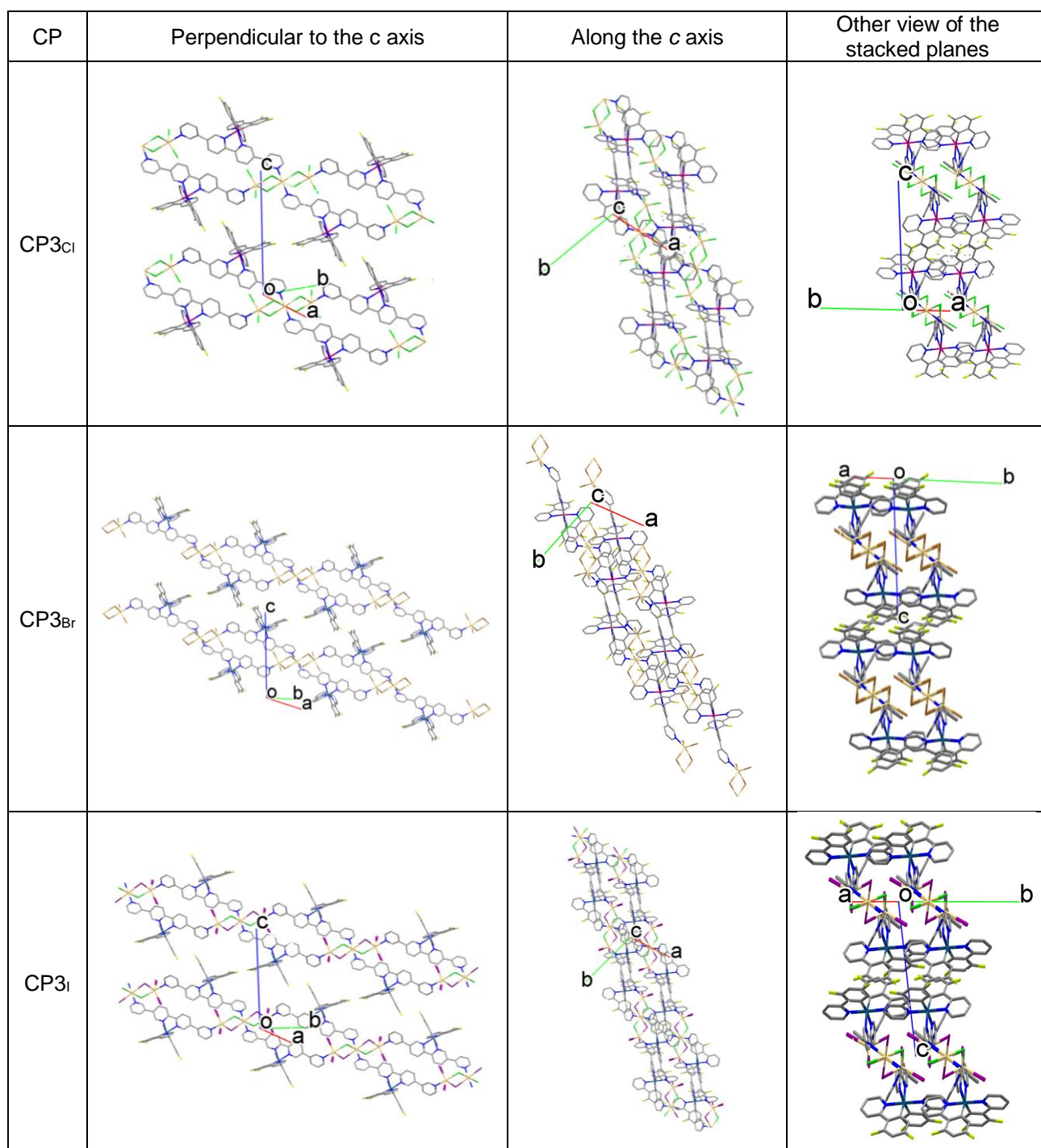


Fig. S11: Portions of the X-Ray structures of **CP3_x** showing the formation of one plane made of parallel 1D coordination polymers represented perpendicular to the *c* axis (a) and stacking of consecutive planes along two distinct directions. For the sake of clarity, only one enantiomer of the Ir complexes has been arbitrary represented even though a statistical distribution of Δ and Λ isomers is observed. H atoms and chloroform solvent molecules have been omitted.

References

1. G. Sheldrick, *Acta Crystallogr., Sect. A*, 2008, **64**, 112-122.
2. G. M. Sheldrick, *Acta Crystallogr., Sect. C*, 2015, **71**, 3-8.
3. A. J. Paterson, S. St John-Campbell, M. F. Mahon, N. J. Press and C. G. Frost, *Chem. Commun.*, 2015, **51**, 12807-12810.
4. J.-F. Ayme, J. E. Beves, D. A. Leigh, R. T. McBurney, K. Rissanen and D. Schultz, *Nat Chem*, 2012, **4**, 15-20.
5. S. Sprouse, K. A. King, P. J. Spellane and R. J. Watts, *J. Am. Chem. Soc.*, 1984, **106**, 6647-6653.
6. Y. You and S. Y. Park, *J. Am. Chem. Soc.*, 2005, **127**, 12438-12439.
7. L. L. Tinker and S. Bernhard, *Inorg. Chem.*, 2009, **48**, 10507-10511.
8. C. Xu, A. Guenet, N. Kyritsakas, J.-M. Planeix and M. W. Hosseini, *Inorg. Chem.*, 2015, **54**, 10429-10439.
9. H. Iranmanesh, K. S. A. Arachchige, M. Bhadbhade, W. A. Donald, J. Y. Liew, K. T. C. Liu, E. T. Luis, E. G. Moore, J. R. Price, H. Yan, J. Yang and J. E. Beves, *Inorg. Chem.*, 2016, **55**, 12737-12751.
10. G. E. Schneider, H. J. Bolink, E. C. Constable, C. D. Ertl, C. E. Housecroft, A. Pertegas, J. A. Zampese, A. Kanitz, F. Kessler and S. B. Meier, *Dalton Trans.*, 2014, **43**, 1961-1964.
11. C. Xu, A. Guenet, N. Kyritsakas, J.-M. Planeix and M. W. Hosseini, *Chem. Commun.*, 2015, **51**, 14785-14788.